M-AM-SymI-1

CHAPERONE-SUBSTRATE INTERACTIONS. **((L. M. Gierasch[1], Z. Wang[2], J. Hunt[2], S. J. Landry[3], E. Feng[1], J. Deisenhofer[2])) [1]Department of Chemistry, University of Massachusetts, Amherst, MA 01003, [2]Howard Hughes Medical Institute, UT Southwestern, Dallas, TX 75235, and [3]Department of Biochemistry, Tulane University Medical Center, New Orleans, LA 70112**

The bacterial Hsp60 molecular chaperone system, GroEL/GroES, facilitates the folding of many different substrate proteins. In order to determine the basis for substrate recognition by GroEL, we have been exploring the interactions of peptide fragments with this chaperone using the development of transferred nuclear Overhauser effects as a measure of binding and a window on the bound conformation. Peptides with a wide range of sequences, including examples that have a high probability of folding as helices or sheets, all can bind GroEL. The unifying property that determines their capacity to bind is their ability to present a hydrophobic surface, regardless of the backbone conformation. This binding mode has implications for the mechanism of GroEL in facilitating protein folding, since it suggests clearly that the chaperone interaction will favor the unfolded state. Furthermore, it is now possible to examine the structure of GroEL and to describe how this binding is achieved by the chaperone. It is additionally important to ask how the co-chaperonin, GroES, acts to drive productive release of substrate from GroEL. We have determined the structure of GroES by X-ray crystallography and analyzed mobile regions of GroES by NMR. The complementary use of these two methods sheds light on the possible function of this co-chaperonin.

M-AM-SymI-2

THE MOLECULAR BASIS OF CHAPERONE-ASSISTED PROTEIN FOLDING

((Sheena E. Radford)) Oxford Centre for Molecular Sciences, University of Oxford, Oxford UK.

Understanding the process of protein folding, during which a disordered polypeptide chain is converted into a compact well defined structure, is one of the major challenges of modern structural biology. In this lecture I discuss how a combination of physical techniques can provide a structural description of the events in the folding of a protein. First, I will discuss how the rapid kinetic events taking place during folding *in vitro* can be monitored and deciphered in structural terms. More detailed structural descriptions of intermediates may be obtained from NMR studies of stable partially folded states will also be addressed. Finally, I will describe how these experimental strategies may be extended in order to relate the findings of *in vitro* studies to the events occurring during folding *in vivo*. The approaches will be illustrated primarily using results from studies of the c-type lysozymes and the homologous α-lactalbumins and their interactions with the chaperonin GroEL.

M-AM-SymI-3

MOLECULAR MECHANISM OF HSP70 CHAPERONES. ((Anthony L. Fink, Daniel R. Palleros, Katherine L. Reid, Micheline Markey and Li Shi)) University of California, Department of Chemistry and Biochemistry, Santa Cruz, CA 95064.

The hsp70 molecular chaperones have been implicated in protein folding, translocation and the heat shock response. The basic paradigm of their function is that they bind unfolded proteins and peptides, which are released on binding and hydrolysis of ATP. The kinetics of binding and dissociation were measured using a fluorescence-labeled unfolded protein. The rates of various steps in the reaction cycle are quite sensitive to the concentrations of nucleotide, K^+ and the protein cofactors DnaJ and GrpE. Using a thermally unstable mutant of staphylococcal nuclease, as well as a permanently unfolded substrate protein, and CD and fluorescence difference spectroscopy, we were able to demonstrate that the bound substrate protein (complex formed at 37 °C where the substrate protein is unfolded) is predominantly unfolded in the complex at temperatures where it would be native in the absence of the chaperone. The addition of ATP dissociated the complex releasing the substrate protein, also in an unfolded conformation. We propose a model for the cycle of interaction of DnaK, the *E. coli* hsp70, with unfolded proteins, in which nucleotides and the protein cofactors play a major role in regulating the cycle.

M-AM-SymI-4

PATHWAYS OF CHAPERONIN-MEDIATED PROTEIN FOLDING.

((U. Hartl)) Memorial Sloan-Kettering Cancer Ctr.

SYNAPTIC TRANSMISSION I

M-AM-A1

MONTE CARLO SIMULATIONS OF MINIATURE SYNAPTIC CURRENTS SUGGEST A STRUCTURAL MECHANISM FOR SYNAPTIC PLASTICITY.

((Piotr J. Kruk and Donald S. Faber)) Department of Anatomy and Neurobiology, Medical College of Pennsylvania, Philadelphia, PA 19129

Monte Carlo simulations of synaptic currents were previously used to demonstrate the contribution of single channel properties to variations in quantal size (*Science* **258**:1494-1498, 1992). The effects of synaptic geometry on the size and kinetics of quanta have been explored with a modified computer model, and we report here a potential structural basis for synaptic plasticity. The model simulates vesicular release of transmitter, random diffusion of the transmitter within and out of the contact zone, and transmitter interactions with the postsynaptic receptor-channel molecules. Simulated events, characterized by the number of open channels versus time, are representative of responses recorded at fast synapses. They reach peak amplitude within 0.5 ms and decay exponentially with a time constant of 3-5 ms. Diffusion, which quickly removes unbound transmitter, can be rate limiting not only for the decay but also for the rising phase and peak amplitude of the miniature events. Responses were simulated with the diameter of the postsynaptic receptor cluster being 0.1-0.5 μm, corresponding to 37-2000 available channels, and for each case the diameter of the contact zone between the presynaptic terminal and postsynaptic membrane was varied from 0.2 to 1 μm. In smaller contact zones the amplitudes were low because diffusion quickly removed the transmitter and left most of the receptors unbound. Bigger contact zones (1 μm diameter) produced significantly larger amplitudes (>100% increase) as transmitter stayed longer in the cleft. Thus, merely increasing the size of a presynaptic bouton or the area in which it is apposed to the postsynaptic cell may result in synaptic potentiation, without any change in transmitter release or in the number or distribution of receptors available for activation.

M-AM-A2

THE CONDUCTANCE OF THE MUSCLE NICOTINIC RECEPTOR CHANNEL CHANGES RAPIDLY UPON GATING.

((D.J. Maconochie, G.H. Fletcher and J.H. Steinbach)) Department of Anesthesiology, Washington University School of Medicine, Saint Louis, MO 63110

In most analyses of channel gating, activation is modelled as a process involving discrete kinetic states with instantaneous transitions between them. However, it is not obvious that the time required for a change in the current flowing through a channel may be considered brief compared to estimates of the time taken for a change in the conformation of the channel protein, in particular the isomerization to the open state. Previous studies of single channel currents recorded from nicotinic receptors at bandwidths of 5 to 10 kHz have indicated that the measured time course of the current when a channel opens or closes is limited by the measuring apparatus (Hamill et al, Pflugers Arch. 391:85-100, 1981). We have recorded single channel currents through fetal-type muscle nicotinic receptor channels expressed in quail fibroblasts, at bandwidths of approximately 50 kHz and 75 kHz. By aligning and averaging the leading or trailing edges of single channel bursts, we obtained an indication of the time course of openings and closings. This measured time course can be entirely accounted for if it is assumed that the conductance of the single channel changes instantaneously, the resulting current signal is modified by the recording apparatus, and alignment and averaging introduce a dispersion of about 3 microseconds. By examining the power spectral density associated with the opening and closing transitions we can exclude the possibility of the transitions following an exponential time course with a time constant of 10 microseconds or longer. Overall, these results indicate that provided the rate of isomerization to the open state does not exceed 100,000 per second, the time taken for the single channel current to change need not be considered a factor in the analysis of activation for this receptor. Supported by grants RO1 NS22356 and PO1 GM47969 to JHS.

M-AM-A3

Correlation between thermodynamic properties of the nicotinic acetylcholine receptor channel expressed in native and heterologous cellular systems and physical state of the membrane in which it is inserted. L.P. Zanello, E. Aztiria, S. Antollini, A.M. Roccamo and F.J. Barrantes. Instituto de Investigaciones Bioquímicas, 8000 Bahía Blanca, Argentina.

The temperature sensitivity of mouse muscle nicotinic acetylcholine receptor (AChR) channel was studied in a) the native embryonic (γ-)AChR in the BC3H-1 clonal cell line, and b) embryonic (γ-) and adult (ε-) forms of the AChR heterologously expressed in CHO cells. Unitary conductance and channel closing rate, α, were measured in inside-out patches over a temperature range from 5° to 35°C. Arrhenius plots obtained for the two AChR types enabled calculation of Q_{10} values of ≈1.2 and 2.0 for the processes of K^+ conductance and channel closure respectively. Using Eyring transition rate theory both γ- and ε-AChR were found to display similar characteristics in all cell types, with relatively low thermal sensitivity of the ionic conductance. Activation energies (E_a) of 3.0-5.0 kcal.mol^{-1} suggest that ions traverse the pore by diffusion. Channel closure showed higher energy requirements, with activation enthalpies of ≈13.5 kcal.mol^{-1} at 20°C. Although γ- and ε-AChRs exhibited similar thermodynamic parameters, a slightly higher E_a value for the conductance and kinetic processes was obtained for the γ-AChR in the heterologous CHO-AR42 cellular system. Fluorescence measurements using the probe Laurdan enabled us to establish a correlation between the electrophysiological and energetic parameters of the AChR proper and the physicochemical properties of the membrane bilayer in which the protein is embedded. All AChRs heterologously expressed in CHO cells were found to be more sensitive than the native γ-AChR in BC3H-1 cells to thermal changes in membrane fluidity. Changes in the physical state of the membrane environment may thus exert subtle but noticeable effects on AChR activity.

M-AM-A4

PRESYNAPTIC BASIS FOR INDUCTION AND EXPRESSION OF HOMOSYNAPTIC DEPRESSION. ((B.A. Armitage and S.A. Siegelbaum)) Columbia Univ., NYC, New York, 10032. (Spon. by L. Zablow)

In the monosynaptic connection between *Aplysia* sensory and motor neurons, homosynaptic depression is a robust phenomenon. In culture, it occurs at every synapse, resulting in a 25-40% decrease in EPSP amplitude in response to the second action potential, even with an interstimulus interval (ISI) of several minutes. Previous quantal analysis suggested that depression was due to decreased transmitter release (Castellucci & Kandel, 1974). We have now extended that study to show that the induction as well as the expression of depression are presynaptic. We first mimicked transmitter release by pressure applying glutamate, (the sensory neuron transmitter), to the co-cultures. Both the EPSP measured with microelectrodes and the EPSC measured with whole-cell voltage clamp was unaltered in response to 5 pulses (100 msec, ISI=1 min). Secondly, we used DNQX to block the postsynaptic response and stimulated the sensory neuron to fire action potentials (5x, ISI=1 min). When the EPSP was measured following washout of DNQX, it was only 20% of the initial response, indicating that presynaptic activity alone was sufficient to cause depression. This result also suggests that presynaptic DNQX-sensitive glutamate receptors do not mediate the changes in transmitter release. Previous models had postulated that depression is partly due to changes in the presynaptic calcium transient. We tested this hypothesis by imaging calcium at presynaptic terminals during a single action potential. In a series of 6 spikes, (ISI=20 sec), the EPSP depressed to an average of 40% of the initial response, whereas the calcium transient showed no significant change (p>0.1, Student's t-test, n=9).

M-AM-A5

KINETIC ANALYSIS OF SYNAPTIC CURRENTS REVEALS A PROLONGED PRESENCE OF GLUTAMATE DURING SYNAPTIC TRANSMISSION TO CEREBELLAR PURKINJE CELLS **((B.U. Keller, B. Barbour, I.Llano and A.Marty))** Zentrum Physiologie, Universität Göttingen, 37073 Göttingen, Germany and Ecole Normale Superieure, F-75005 Paris, France.

AMPA/KA receptor mediated excitatory postsynaptic currents (EPSCs) were recorded in cerebellar Purkinje cells and interneurons by using patch clamp recordings in thin slices. AMPA/KA receptor mediated EPSCs decayed much more slowly in Purkinje cells than those recorded in interneurones. The slowness of the Purkinje cell EPSCs did not result from dendritic filtering and did not reflect the deactivation kinetics of the AMPA/KA receptors. Instead, comparison of EPSC and AMPA/KA receptor kinetics suggested that the slow EPSC decay in Purkinje cells resulted from the prolonged presence of glutamate during synaptic transmission. This may be due to retarded transmitter diffusion around Purkinje cells or to cross - talk between neighboring synapses.

M-AM-A6

ALTERING $GABA_A$ CHANNEL DESENSITIZATION SHORTENS IPSC DURATION ((M.V. Jones and G.L. Westbrook)) The Vollum Institute for Advanced Biomedical Research, Portland, OR 97201 (Spon. G.L. Westbrook)

The time course of $GABA_A$ receptor-mediated inhibitory postsynaptic currents (IPSCs) influences signaling in brain regions featuring inhibitory circuitry. We studied responses to controlled GABA pulses and to synaptic release of GABA, and found that increasing macroscopic desensitization shortens the IPSC time course.

Whole-cell and outside-out patch recordings (25°C) were made from rat hippocampal neurons in culture, using CsCl-based pipette solutions containing either 5mM Mg_2ATP or $Li_4ATP\gamma S$. Cells and patches were continuously perfused with NaCl-based external solution, and rapid applications (Clements et al., *Science* 258:1498) of GABA were made with a solution exchange time of ~1ms.

Short pulses of GABA (1-5ms, 1-10mM) to outside-out patches activated bicuculline-sensitive chloride currents that had biexponential decays (mean time constants: τ=30 and 254ms, n=13). Spontaneous IPSCs also decayed biexponentially (τ=18ms (50% of amplitude), 104ms, n=9 cells). Desensitization occurred during long (100ms) pulses (τ=7ms, 130ms, n=8), and also after short pulses as measured by paired-pulse depression. Recovery from paired-pulse desensitization (τ=61ms, n=3) overlapped with the current decay after a single short pulse, showing that both entry and recovery from desensitized states occur during decay after short pulses. Replacing ATP with ATPγS increased long pulse desensitization (τ=4ms, 48 ms, n=4; Fig.1) and slowed recovery from short pulse desensitization (τ=~350ms, n=2). ATPγS also increased the rate of decay after short pulses (τ=14ms, 147ms, n=9) and caused IPSCs to be dominated by the fast decay component (τ=16ms (82%), 86ms, n=7; Fig.2). These data suggest that fast recovery from desensitization prolongs IPSC decay, and that regulation of desensitization may therefore be a strategy for modulating the duration and frequency dependence of inhibition.

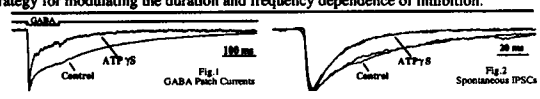

K^+ CHANNELS I

M-AM-B1

EXPRESSION OF AN EPITHELIAL CA^{2+}-ACTIVATED K^+ CHANNEL IN *XENOPUS LAEVIS* OOCYTES. ((D.A. Klærke*#, M. Markussen*, H. Wiener+, T. Zeuthen#, and P.L. Jørgensen*)) Biomembrane Research Centre, *August Krogh Institute and #Dept. of Medical Physiology, University of Copenhagen, Denmark; +Dept. of Pharmacology, University of Vienna, Austria. (Spon. by S. Dissing)

Ca^{2+}-activated K^+ channels in the basolateral membrane of surface cells in the rabbit distal colon are important for regulation of the transepithelial ion transport. These cells are responsible for hormone regulated Na^+ reabsorption from the intestinal lumen and the basolateral K^+ conductance is increased after aldosterone stimulation. The molecular structure for epithelial Ca^{2+}-activated K^+ channels is not known. To express Ca^{2+}-activated K^+ channels in *Xenopus laevis* oocytes, poly(A$^+$)RNA has been isolated from the distal colon of rabbits kept for 48 hours on a low sodium diet to increase their endogenous level of aldosterone. App. 50 ng poly(A$^+$)RNA is injected into each oocyte and after incubation for 3 days, K^+ channel activity measured as Ba^{2+}-sensitive $^{86}Rb^+$ uptake into whole oocytes is increased up to 5 fold. The Ca^{2+}-sensitivity of the expressed channels cannot be determined in whole oocytes, since it is impossible to control the intracellular Ca^{2+}. To obtain single channel measurements of expressed K^+ channels, plasma membrane fractions prepared from batches of injected oocytes are fused with planar lipid bilayers. These experiments show expression of a maxi K^+ channel with a single channel conductance of 250-300 pS. The channel is Ca^{2+}-dependent and sensitive to Charybdotoxin (100 nM). Our results show that Ca^{2+}-activated K^+ channels from rabbit distal colon can be expressed in a functional state in *Xenopus laevis* oocytes.

M-AM-B2

CLONING AND FUNCTIONAL EXPRESSION OF A HUMAN CA-DEPENDENT MAXI K CHANNEL (*hSlo*). ((M. Wallner, P. Meera, M. Ottolia, and L. Toro)). UCLA, Los Angeles, CA, 90024.

A cDNA-fragment of the conserved C-terminus (mouse/*Drosophila*) was amplified by PCR from mouse brain RNA, cloned and used as hybridization probe for Northern blots. Two major bands were detected (6 kb and 12 kb). The 6 kb transcript is predominant in myometrium, aorta, coronary and intestine; whereas in mouse brain, the 12 kb transcript predominates. The highest abundance of mRNA was found in human myometrium. cDNA clones were isolated from cDNA libraries made from this tissue. We found a novel splice variant at splice site A which was present in two out of five clones. Excluding splice variations, the amino acid identity is 99.7% when compared with the mouse sequence, indicative that we have isolated the human homologue (*hSlo*). An interesting feature of the *hSlo* clone are two stretches of GC-rich triplet repeats at the 5'-end located between putative start codons. Elongation of similar sequences are the cause of genetic diseases like fragile X syndrome and Huntington disease. As expected from the genetic instability of this type of triplet repeats, sequence alignment with the mouse clone shows variability in the length of each of these repeats. Functional expression of full length constructs in *Xenopus laevis* oocytes displayed characteristics typical of "maxi" K channels, including single channel conductance, calcium sensitivity and pharmacology. Supported by NIH HL47382, GM50550.

M-AM-B3

DIFFERENTIAL EFFECTS OF THE 'MAXI K' β SUBUNIT ON THE α SUBUNIT OF HUMAN AND *DROSOPHILA* EXPRESSED IN *XENOPUS LAEVIS* OOCYTES. ((P. Meera*, M. Wallner*, M. Ottolia*, J. P. Adelman†, G. Kaczorowski§, M. L. Garcia§, and L. Toro*)). *UCLA, Los Angeles, CA 90024. §Merck Res. Labs., Rahway, NJ 07065. †Oregon Hlth. Sci. Univ. Portland, OR 97201.

We have studied the effect of the 'MaxiK' β-subunit cloned from bovine trachea (Knaus *et al*, *JBC*, 269:17274, 1994) on the α-subunit of human *Slo* (*hSlo*) (Wallner *et al*, this meeting) and *Drosophila Slo* (*dSlo*) (A1C2E1G3I0 variant, Adelman *et al*, *Neuron*, 9:209, 1992) by heterologous expression in *Xenopus laevis* oocytes. The α-subunit alone is sufficient to form functional channels, however when coexpressed with the β-subunit its activation curve (in 10 μM Ca^{2+}) was shifted to more negative potentials. In *hSlo* alone, the half activation potential ($V_{½}$) was 17.5 ± 19 mV, but when co-expressed with the β-subunit this value was shifted by -100 mV ($V_{½-α+β}$ = -83 ± 9 mV) ($p \leq 0.001$). Whereas $V_{½}$ in *dSlo* was only shifted by -17 mV ($V_{½-α}$ = 17 ± 23, n = 21 and $V_{½-α+β}$ = 0.2 ± 21, n = 21, $p \geq 0.02$). In agreement with our previous findings in bilayers (Pérez et al, *Biophys. J.* 66:1022, 1994), $V_{½}$ values have a large standard deviation even when studied in the same oocyte. The effective valence (zδ), on the other hand, remained practically the same when both clones were analyzed. For *hSlo* α subunit, zδ was 1.76 ± 0.3, and for α + β subunits was 1.67 ± 0.3; for *dSlo* α subunit, zδ was 1.37 ± 0.4, and for α + β subunits was 1.21 ± 0.3, indicating that the majority of the channels were associated with the β subunit. This association was also evident after channel incorporation into lipid bilayers. Injection of β-subunit alone in oocytes yielded no currents. In conclusion, our studies reveal that the β subunit strongly modulates *hSlo* whereas the modulation of *dSlo* is weak. Supported by NIH HL47382, GM50550.

M-AM-B4

RATE-LIMITING STEPS IN CALCIUM-ACTIVATION OF BK CHANNELS. ((Brad S. Rothberg, Lu Song and Karl L. Magleby)) Dept. of Physiology and Biophysics, Univ. of Miami School of Med., Miami, FL 33101

The major features of the Ca-dependent gating of large conductance calcium-activated K^+ (BK) channels can be described by a kinetic scheme with three open and five shut states (McManus and Magleby, J.Physiol. 443:739-777, 1991). In this scheme, the rate constants for the Ca-dependent transitions are multiplied by [Ca]i, resulting in decreases in the mean lifetimes of the longer closed states with increasing [Ca]i. A prediction of this scheme, therefore, is that both the time constants and relative areas of the longer components of shut-interval distributions will continue to decrease as [Ca]i is increased. To evaluate this prediction, single channel currents were collected by patch clamp recording from BK channels in cultured rat muscle over a 1000-fold range of [Ca]i. Popen and dwell-time distributions of experimental data were then compared to distributions predicted by the kinetic scheme using rates determined *via* Q-matrix methods. While the kinetic scheme correctly predicted channel activity for low [Ca]i (<20 μM), predictions for high [Ca]i (>20 μM) gave time constants and areas for the longer shut components which decreased to a much greater extent than those observed experimentally. The reduced experimental response may reflect an apparent saturation of the Ca-binding steps. We can account for this apparent saturation in Ca-binding by replacing each Ca-binding step in the previous scheme with a two-step reaction: in the first step Ca binds to the binding site and in the second step the binding induces a conformational change. Supported by Grants from the NIH and Muscular Dystrophy Association to K.L.M.

M-AM-B5

SLOW GATING PROCESSES CAN MODULATE ACTIVITY OF A CLONED CA^{2+}-ACTIVATED K^+ (BK) CHANNEL ((Shai D. Silberberg*, Armando Lagrutta+, John P. Adelman+, and Karl L. Magleby#)) *Dept. Life Sciences, Ben Gurion Univ. of the Negev, Beer-Sheva 84105, +Vollum Institute, Oregon Health Sciences Univ., Portland Oregon 97201, and #Dept. of Physiology and Biophysics, Univ. of Miami School of Med., Miami, FL 33101

Large conductance Ca-activated K^+ channels (BK channels) from the same tissue can display large differences in Popen for a given [Ca]i (McManus and Magleby, 1991; *J. Physiol.* 443, 739-777). Such variability could arise if the channels have different primary structures due to alternative splicing (Adelman et al. 1992, *Neuron* 9:209-216). If the variability arises exclusively from different alternative splicing, then it should be eliminated when cloned channels of the same type are examined. This possibility was tested by expressing in Xenopus oocytes the cloned *Drosophila Slo* BK channel A1/C2/E1/G3/I0 or a mutated form of this channel in which serine is changed to alanine (S942A) to eliminate a putative PKA phosphorylation site. In contrast to the prediction, we found that the differences in Popen among channels of the same type for a given [Ca]i were still present, and this was the case for both the cloned and mutated channels. In addition, we found that both the cloned and mutated channels usually displayed a slow gating process with a time course of seconds to minutes that modulated channel activity to produce large fluctuating changes in Popen. The variable Popen associated with the slow gating process resulted mainly from changes in the frequencies and durations of the longest shut intervals, with only minor changes in the open intervals. It is unclear whether the variability arises from intrinsic properties of the channels or from associated membrane and/or cytoplasmic factors. Supported by Grants from the NIH (AR32807 and NS31872), the Muscular Dystrophy Association, and the BSF 93-00061/1.

M-AM-B6

HETEROTETRAMER FORMATION AND CHARYBDOTOXIN SENSITIVITY OF TWO K^+ CHANNELS CLONED FROM SMOOTH MUSCLE. ((Scott N. Russell, Kenneth E. Overturf and Burton Horowitz)) University of Nevada, Department of Physiology, Reno, NV 89557

Delayed rectifier K^+ channels are involved in the electrical activity of all excitable cells. The relationship between native K^+ currents recorded from these cells and cloned K^+ channel cDNAs has been difficult to ascertain partly because of contradictions in pharmacological characteristics between native and expressed currents. By studying the charybdotoxin (CTX) pharmacology of two cloned, smooth muscle delayed rectifier K^+ channels ($cK_v1.2$ and $cK_v1.5$) expressed in oocytes, evidence for heterotetramer formation was obtained. We have shown that the presence of even a single CTX insensitive subunit renders the heterotetrameric channel insensitive to CTX. The two K^+ channel clones differ in an amino acid at the mouth of the pore region which may be in a position to block the access of CTX to its binding site, and hence determine CTX sensitivity of the heterotetrameric channel. These results may explain discrepancies reported between native and cloned smooth muscle K^+ channels.

M-AM-B7

MODIFICATION OF ION CHANNELS BY ULTRAVIOLET LIGHT. ((T.R. Middendorf[1], C. Adams[2], D.A. Baylor[1], and R.W. Aldrich[2]))
[1]Dept. of Neurobiology and [2]Dept. of Molecular and Cellular Physiology and Howard Hughes Medical Institute, School of Medicine, Stanford University, Stanford, CA 94305.

We have used *in situ* UV modification of cloned channels to probe the role of aromatic amino acids in ion channel function. UV irradiation of excised membrane patches of *Xenopus* oocytes expressing either voltage-activated *Shaker* potassium channels or cGMP-activated rod channels caused a dose-dependent, irreversible decline in patch current, consistent with permanent chemical modification of amino acids in the channel. In *Shaker* channels, the kinetics of activation were also significantly slowed by UV exposure. By employing excitation wavelengths longer than 250 nm, the effect of UV light was restricted to the aromatic amino acids Trp, Tyr, and Phe. A comparison of the wavelength dependence of the UV sensitivity (the action spectrum) with the absorption spectra of the aromatic amino acids suggests that current knockout is initiated by Trp absorption. The dependence of the fractional knockout on photon dosage for the cGMP-activated channel implies that modification of a small subset of the channel Trp residues is sufficient for current knockout, and that the mechanism of knockout is the same for all wavelengths from 250 nm-330 nm. The sensitivity of the channels to UV light was similar for patches exposed to the same number of photons from a pulsed laser or a dc arc lamp, suggesting that photochemical modification proceeded by a one-photon process. Mutagenesis is being employed to identify the specific amino acid residue(s) whose modification leads to the current loss. (Supported by EY01543, EY06351, and Howard Hughes Medical Institute.)

M-AM-B8

CLONING AND FUNCTIONAL EXPRESSION OF A NOVEL K^+ CHANNEL β-SUBUNIT FROM HUMAN ATRIUM ((K. Majumder, M. DeBiasi, Z. Wang, and B.A. Wible)) Dept. of Molecular Physiology and Biophysics, Baylor College of Medicine, Houston, Tx 77030.

The recent cloning of a K^+ channel β-subunit from rat brain, $K_v\beta1$, which accelerates the inactivation kinetics of channels in the K_v1 subfamily of voltage-gated K^+ channels (Rettig et al, *Nature* 369: 289-294 [1994]) prompted us to search for the expression of β-subunits in human heart, a tissue which expresses a diversity of voltage-gated and inwardly rectifying K^+ channels. We screened an adult human atrial cDNA library for sequences homologous to bovine brain $K_v\beta2$, and isolated a full-length clone which, in a single open reading frame, predicts a 408 amino acid protein highly homologous to the other $K_v\beta$-subunits. This cDNA, $hK_v\beta3$, represents a third β-subunit isoform, however. The N-terminal 79 residues of $hK_v\beta3$ are essentially unique, while the remaining 329 amino acids are 85 to 100% identical to the other $K_v\beta$ sequences. Upon heterologous expression in *Xenopus* oocytes, we found that $hK_v\beta3$ modifies only coinjected $hK_v1.5$ and $hK_v1.4$ currents. Specifically, $hK_v\beta3$ accelerates the inactivation of $hK_v1.4$ currents two to three fold, and induces fast inactivation of non-inactivating $hK_v1.5$ currents at potentials ranging from +30 to +80 mV. In addition, both channels showed accelerated activation kinetics in the presence of $hK_v\beta3$. By contrast, $hK_v\beta3$ had no effect on heterologously expressed $hK_v1.1$, $hK_v1.2$, $hK_v2.1$, or the inward rectifiers IRK1 or hIRK (cloned from human heart). Thus, we have cloned a third type of K^+ channel β-subunit which affects only a subset of the K_v1 subfamily channels. Supported by HL37044 to B.A.W. and HL36930 to A. M. Brown.

M-AM-B9

CLONING AND EXPRESSION OF A NOVEL K+ CHANNEL ß-SUBUNIT FROM FERRET VENTRICLE ((M.J. Morales, R.L. Rasmusson, R.C. Castellino, A.L. Crews and H.C. Strauss)) Duke University Med. Ctr., Durham, NC 27710.

Recently, a ß-subunit (Kvß1) which modifies inactivation of Kv1.1 and Kv1.4 channels was isolated from rat brain (Rettig et al. 1994. Nature 369, 289.). Kvß1 mRNA was detected exclusively in brain. To determine if other K+ channel ß-subunits might be found in cardiac tissue we attempted to clone these proteins from heart. PCR primers were used to amplify a 440 bp DNA fragment from ferret right ventricle cDNA. Sequence analysis showed that this fragment had extensive similarity to a previously described ß-subunit. The 440 bp fragment was labelled and used as a probe to screen a ferret ventricular cDNA library. A positive clone was identified and sequenced. The cDNA, designated Kvß3, has a 408 amino acid open reading frame. Sequence analysis revealed that ferret Kvß3 is identical to rat Kvß1 over the 329 C-terminus amino acids. However, there is no similarity among the first 72 amino acids of the ferret Kvß3 subunit and rat Kvß1. There is no significant similarity between the N-terminus of ferret Kvß3 and any other protein sequence. Despite their apparent lack of similarity, the N-termini of Kvß1 and Kvß3 share one potentially important structural feature: a cysteine residue near the N-terminus. Kvß3 also shares an important functional similarity to Kvß1, in that it increases the rate of fast inactivation of Kv1.4 when coexpressed in *Xenopus* oocytes. Cross species PCR using oligonucleotides which are complementary to the unique portion of the ferret cDNA was performed on rat and human cDNA and yielded the expected 400 nucleotide DNA species which were cloned and sequenced. Kvß3 was present in both human and rat showing 88% and 80% conservation in the N-terminal region with ferret Kvß3.

RNA/DNA STRUCTURE

M-AM-C1

THREE-DIMENSIONAL LATTICE STRUCTURES FOR A MINIMAL HAMMERHEAD RIBOZYME. ((Brooke Lustig, Robert L. Jernigan and Kuan-Teh Jeang*)) Laboratory of Mathematical Biology, NCI, NIH, Bethesda, MD, 20892. *Laboratory of Molecular Microbiology, NIAID, NIH, Bethesda, MD, 20892.

Computational methods using lattices have been successful in the generation and evaluation of three-dimensional structures of t-RNA.[1] These methods predicted the native tertiary pairs and their stem stacking arrangement as well as alternative tertiary pairs found consistent with experiment. Some of the approaches are applied here to another small RNA, an extensively mutagenized hammerhead ribozyme. Progressive mutagenesis has shown that one of the three original stems and its attached hairpin loop are not essential for catalysis. This minimal hammerhead requires, for significant catalytic activity, a G in a particular sequence position. We have generated exhaustively about 87 million three-dimensional representations for this ribozyme, and found a major class of structures with the requisite G proximate to the cleavage site. There is a strong correlation between stem stacking and placement of that G in a particular orientation relative to the cleavage site. This orientation is the result of the asymmetry in length of two sections of internal loop.

1. Lustig, B., Covell, D. G. and Jernigan, R. L. (1994) *J. Biomol. Struct. Dyn. 12*, 145.

M-AM-C2

SOLUTION STRUCTURE OF THE SPLICED LEADER RNA FROM *C. elegans*. ((Nancy L. Greenbaum*, Ishwar Radhakrishnan*, Dinshaw J. Patel+, and David Hirsh*)) *Department of Biochemistry and Molecular Biophysics, Columbia University, New York, NY 10032, and +Cellular Biophysics and Biochemistry Program, Sloan Kettering Institute, New York, NY 10021. (spon. by W.A. Hendrickson)

Trans-splicing involves the ligation of two independent RNA molecules into a single transcript, and is a required process in the maturation of mRNAs of several organisms. In nematodes, *trans*-splicing results in the transfer of a 22-nucleotide 5' exon from the spliced leader (SL) RNA to a 3' concensus acceptor site of a separate pre-mRNA. All known SL RNAs are thought to fold into a structure containing three stem loops. The first stem loop contains both the 5' splice donor site and a complementary base-paired region reminiscent of the pairing of the 5' splice site and U1 snRNA in the chemically analogous process of *cis*-splicing. The structure of the first stem loop of the SL1 RNA of *C. elegans* has been studied by homonuclear and heteronuclear NMR techniques. The stem is an A-form helix, typical of RNA. Sequential connectivities throughout the nine-nucleotide loop and long-distance NOE's suggest that the loop folds into a unique and stable structure with the possibility of additional hydrogen bonds. The first part of the loop continues the A-type helical conformation. A turn occurs at a guanosine residue in a *syn* conformation. The final residue of the loop, an adenine flanked by two guanosines immediately 3' to the splice site, is rotated out from the loop-helix junction.

M-AM-C3

A GEOMETRICAL APPROACH IN FOLDING A PSEUDO-KNOT STRUCTURE WITHIN THE E. COLI 16S-RNA. ((C.-S. Tung)) Theoretical Biology and Biophysics, LANL, Los Alamos, NM 87545

Except for tRNA, the tertiary structure of RNA molecules are very little known. The many possibilities in the arrangement of different helices in the space and the flexibility in the single-stranded loops that connect the helical regions make the modeling of the tertiary structure of RNA molecule a very complex task. Here, we introduce a new approach to fold RNA tertiary structure based only on the information of the secondary structure and the stereochemistry of the molecule. This approach was tested by constructing an atomic model of a pseudo-knot (bases 500-545) in the E. coli 16S RNA. The resulting structure (as shown in the figure) is a closely packed molecule that satisfied both the constraints (secondary structure and stereochemistry) as imposed on the molecule.

M-AM-C4

PREDICTING DNA STRUCTURE IN CRYSTALS AND GENOMIC SEQUENCES. ((G. P. Schroth, B. Basham, T. F. Kagawa, M. L. Howell, and P. S. Ho)) Dept. of Biochemistry and Biophysics, Oregon State University, Corvallis, OR 97331

One of the seemingly unapproachable goals in biophysics is the ability to predict the 3-dimensional structure of a biopolymer from sequence information. We have developed a set of thermodynamic models to accurately predict the ability of DNA sequences to adopt the double-helical conformations of A-, B-, and left-handed Z-DNA. We show that the ability of an oligonucleotide sequence to crystallize as Z-DNA can be predicted from the differences in the solvent free energy (SFE) for hydrating that sequence, and that this difference can be used to predict the crystallization pathway and solutions for Z-DNA oligonucleotides. Using an analogous comparison of SFEs for the right-handed duplexes, we have developed a triplet-code to predict whether a sequence will crystallize as A- or B-DNA. This code correctly assigned 88% of all A- and B-DNA crystal structures in the current crystallographic data base.

How do we use this data to understand the biology of DNA secondary structure? The ability of a sequence to undergo a transition from standard B-DNA to either A- or Z-DNA is dependent on the free energy difference between the conformations. We use transition free energies in a statistical mechanics model to predict the formation of Z-DNA in negatively supercoiled DNA of simple sequences, and of sequences found in eucaryotic transcription promoters. We have extended this thermodynamic analysis to map potential Z-DNA forming sequences in over 100 genes of the human genome, and find that Z-DNA sequences cluster at and near the transcription start sites of human genes. We interpret this in terms of the ability of Z-DNA, and other underwound structures, to modulate supercoiling energy resulting from the mechanism of transcription.

M-AM-C5

ENERGY TRANSFER TO 2-AMINOPURINE IN DNA REFLECTS BASE-SPECIFIC INTERACTIONS† ((D. Xu, K.O. Evans and T. M. Nordlund)) Dept. of Physics, University of Alabama at Birmingham, Birmingham, AL 35294-1170

The efficiency of energy transfer from normal bases to a 2-aminopurine (2AP) base incorporated near the center of oligonucleotides has been determined as a function of base sequence near the fluorescent base. In the duplex decamer d(CTGA[2AP]TTCAG)$_2$, we have reported a maximum overall transfer efficiency from normal bases to 2AP of 4-5% near 0 °C.[1] The temperature dependence of transfer reflects helix premelting behavior.[2] For single-stranded d(AAAA[2AP]AAAAA), the overall efficiency of transfer is near 46%; for analogous decamers with C, T, or G in place of A, the efficiency is an order of magnitude lower. These results imply (i) that transfer in the decamer d(AAAA[2AP]AAAAA) occurs from 4 or more bases and (ii) that the transfer in the d(CTGA[2AP]TTCAG)$_2$ duplex decamer is almost entirely due to a highly efficient transfer from the adjacent A. In s-s d(AAAA[2AP]AAAAA), unlike the other decamers, A shows strong stacking interaction with 2AP. Fluorescence and absorption spectra of d(GGGG[2AP]GGGGG) reveal that G also has a strong electronic interaction with 2AP, but that this is not a stacking interaction. It appears, then, that strong stacking interaction facilitates energy transfer along the DNA helix and that appreciable transfer occurs only when adenine is next to 2AP. Detailed sequence dependence of spectra and transfer will be presented.

† Supported in part by NSF grant DMB 9118185.

1. T. M. Nordlund, D. Xu, K. O. Evans, *Biochemistry* **32**, 12090-95 (1993).
2. D. Xu, K. O. Evans, T. M. Nordlund, *Biochemistry* **33**, 9592-99 (1994).

M-AM-C6

STACKING FREE ENERGY PROFILES FOR ALL 16 NATURAL RIBODINUCLEOSIDE MONOPHOSPHATES IN AQUEOUS SOLUTION ((J. Norberg and L. Nilsson)) Karolinska institutet, Center for Structural Biochemistry, NOVUM Research Park, S-141 57 Huddinge, Sweden.

The phenomenon of base stacking, which we treat here in full atomic detail for RNA fragments including solvent and the sugar phosphate backbone, is not yet completely understood. We present free energy profiles of stacking for all 16 natural ribodinucleoside monophosphates based on potential of mean force calculations. Stacking preferences follow the general sequence purine/purine > purine/pyrimidine > pyrimidine/pyrimidine with the stacked state having several kcal/mol lower free energy than the unstacked states for purine-purine combinations. In energetic terms neither the total energy of the dinucleotides, nor the base-base interaction energy, has a direct correspondence to the potential of mean force even though they show the same overall trend. We find that the two other energetic components, involving backbone and solvent, are of the same magnitude as base-base interactions, but not with the same sequence dependence.

M-AM-C7

SALT AND TEMPERATURE INDUCED CONFORMATIONAL CHANGES OF TWO SELF COMPLEMENTARY DODECANUCLEOTIDES. ((I. Haq[1], S.J. Senior[1], A.F. Drake[2], S. Leharne[1], T.C. Jenkins[3] and B.Z. Chowdhry[1])) [1]The University of Greenwich, London; [2]Birkbeck College, The University of London; and [3]Cancer Research Campaign, Sutton Surrey, UK.

The salt and temperature dependent conformational behaviour of two self complementary dodecanucleotides with AT-rich core base tracts, (A2T2 and A3T3), have been examined using HSDSC, UV-VIS spectrophotometry, and CD. We have established that both sequences can adopt a single-stranded hairpin-type conformation, particularly under low salt concentrations, although these forms undergo thermally induced structural transitions at relatively low temperatures. In contrast to earlier reports for A2T2, neither oligomer duplex shows monophasic temperature dependent melting behaviour, as monitored either calorimetrically or optically, and in each case there is clear evidence for a premelting transition. The qualitative effects of added salt upon the stabilities of both the hairpin monomer and duplex structures have been examined. A qualitative model for the different conformational, dynamic and thermodynamic behaviours of these $(A/T)_n$ containing sequences will be described.

M-AM-C8

CHANGES IN STRUCTURE OF DNA, IONS AND WATER INDUCED BY A CYCLOBUTANE THYMINE DIMER. ((R. Osman[1], N. Luo[1], K. Miaskiewicz[2])) [1]Physiology & Biophysics, Mount Sinai School of Medicine, New York, NY 10029; [2]Pacific Northwest Laboratories, Richland, WA 99352 (Spon. by R. Osman)

Molecular dynamics simulations of the dodecamer d(CGCGAATTCGCG)$_2$ with and without a *cis,syn*-cyclobutane thymine dimer (TD) were conducted with the AMBER force field on a system containing the DNA, 22 Na^+ ions and 1538 water molecules in a box with periodic boundaries. Analysis of the structural changes in the damaged DNA shows that the distortions are localized near the 5'-thymine of TD and are reflected in a kinked helical axis, a *high anti* orientation of the base, a significantly less mobile sugar of the 5'-thymine of TD, and a disruption of hydrogen bonds to the TD. A wider minor groove in the vicinity of the lesion contributes to an increased distance between the 5'-thymine of the dimer and the adjacent adenine of the damaged strand. These results are in very good agreement with available NMR data. Comparison of the distribution of counterions in normal and in damaged DNA shows a depletion in the minor groove in a 5'-direction to the thymine dimer and in the major groove in the vicinity of the lesion. Examination of the structure of water in the grooves of DNA shows significant disruption of the spine-like hydrogen bonding in the minor groove, in particular in the vicinity of the lesion. Similar but smaller changes are also observed in the major groove. The importance of the changes in DNA structure, and in particular in the counterion and water distribution in the minor groove, are highlighted by the observation that the repair enzyme endonuclease V binds specifically to TD-containing DNA in the minor groove.

Supported by USDOE grant DE-FG02-88ER60675.

M-AM-C9

Biological Implications of the Hairpin Structures Formed By The Single Strands of The Fragile-X DNA Triplets. *Xian Chen[1,2], S. V. Santhana Mariappan[1], Paolo Catasti[1,2], Robert Ratliff[2], Robert K. Moyzis[3], Ali Laayoun[5], Steven S. Smith[5], E. Morton Bradbury[2,4] and Goutam Gupta[1]*•. [1]Theoretical Biology and Biophysics, [2]Life Sciences Division, [3]Center for Human Genome Studies, Los Alamos National Laboratory, Los Alamos, NM 87545, [5]Department of Cell and Tumor Biology, City of Hope National Medical Center,Duarte, CA 91010.

The structural and enzymological data lead to two major conclusions regarding the nature of expansion and methylation of the fragile-X triplet repeats, (GGC)n•(GCC)n. (i) Both the C- and G-rich strands of the repeat can independently form hairpins under physiological conditions. However, the C-rich strand has a much higher tendency to form hairpins and therefore, is more likely to form slippage structure and be preferentially expanded during replication. (ii) The hairpins of the C-rich strands display exceptionally high substrate efficiency for the human methyl transferase (6 times higher than the Watson-Crick duplex). This observation provides molecular mechanism of the methylation of the CpG island inside the fragile-X repeat that inactivates the FMR-1 gene and causes the disease.

Based on these data, we propose a model (Figure 1) to explain how hairpin formation by the C-rich strand gives rise to slippage during replication. This leads to both expansion and methylation of the C-rich strand. Finally "maintenance methylation" step causes late replication which may result in defective DNA condensation and fragility.

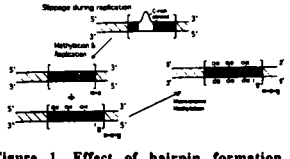

Figure 1. Effect of hairpin formation by the C-rich strand of the fragile-X repeat of length, n=a.

M-AM-D1

BINDING STUDIES OF RUTHENIUM (II) AMMINES TO NUCLEIC ACIDS. ((Edgardo J. Mantilla, Debi Murtha, Wyatt R. Murphy, Jr., Daniel H. Huchital & Richard D. Sheardy)) Department of Chemistry, Seton Hall University, South Orange, NJ 07079.

A series of ruthenium (II) complexes of general formula $[Ru(NH_3)_4]_x(BL)^{+2x}$, where x = 2 for BL = dpp (2,3-bis(2-pyridyl)pyrazine), dpq (2,3-bis(2-pyridyl)quinoxaline) or dpb (2,3-bis(2-pyridyl)benzo[g]quinoxaline) and x = 1 for BL = phen (1,10-phenanthroline), have been synthesized for comparative DNA binding studies. The interactions of these compounds with calf thymus DNA have been investigated by spectrophotometric titrations, equilibrium dialysis and viscometry. For BL = dpb or phen, the changes in λ_{max} and ε_{max} for the $\pi \rightarrow \pi^*$ transitions are consistent with an intercalative mode of interaction for the aromatic moieties of these complexes into the base pairs of DNA. Current work is focusing on the influence of [NaCl] on the binding isotherms for all complexes. Preliminary results for the dpb complex indicate that around 80% of the binding free energy is due to electrostatic interactions. The authors acknowledge NIH Grant GM51069-1 for supprt of this work.

M-AM-D2

SIMULTANEOUS BINDING OF AN INTERCALATING AND GROOVE BINDING DRUGS TO A DEOXYOLIGONUCLEOTIDE

Dongchul Suh and Jonathan B. Chaires
Department of Biochemistry, The University of Mississippi Medical Center, 2500 North State Street, Jackson, MS 39216-4505.

The mutual effect of binding of an intercalating and a groove binding drug at contiguous DNA sites has been studied. A 14-bp deoxyoligonucleotide

5' C-A-G-A-G-C-A-G-T-T-T-T-A-G
3' G-T-C-T-C-G-T-C-A-A-A-A-T-C

was designed, synthesized, and used for binding studies. The sequence contains a specific site for Hoechst 33258. The energetics of the binding of Hoechst 33258, and the intercalators ethidium, daunomycin, and 7-amino-actinomycin were determined by fluorescence titration studies. Bound Hoechst 33258 was found, in all cases, to reduce the binding free energies for the interaction of intercalators with the deoxyoligonucleotide. Coupling free energies for the system were found to range from 0.14 to 0.27 Kcal/mol. Fluorescence resonance energy transfer experiments were used to show that Hoechst 33258 and the various intercalators were bound simultaneously to contiguous sites on the deoxyoligonucleotide. (Supported by N.I.H. Grant CA 35625 (J.B.C.))

M-AM-D3

TELOMERIC DNA:RNA HYBRID DUPLEXES CAN COEXIST IN A HYBRID-DNA TETRAPLEX EQUILIBRIUM THAT IS TEMPERATURE AND CATION DEPENDENT ((Miguel Salazar, Sean M. Kerwin and Laurence H. Hurley)) Drug Dynamics Institute and Dept. of Medicinal Chemistry University of Texas at Austin, Austin TX 78712 (Spon. by D. G. Rhodes)

Telomerase is a specialized reverse transcriptase containing an internal RNA template for synthesis of telomeric DNA. A DNA:RNA hybrid duplex is formed from the telomerase RNA template and the extended telomere. This hybrid duplex then undergoes a translocation step followed by rehybridization in order to continue telomerase synthesis of telomeric DNA. We have discovered an unusual property of telomeric DNA:RNA hybrid duplexes in the d(GGTTAGGGTTAG):r(cuaacccuaacc) hybrid containing the human telomere repeat $d(TTAGGG)_n$ and the telomerase RNA template r(cuaacccuaac). The DNA strand of this hybrid forms a tetraplex structure in solution at room temperature whereas the RNA strand behaves as a normal single stranded oligonucleotide. However, upon addition of the DNA strand to the single stranded RNA, the DNA tetraplex structure unfolds to form a DNA:RNA hybrid duplex. This hybrid duplex is relatively stable at room temperature in buffers containing either sodium or potassium cations, but it behaves differently with increasing temperature in these two ionic conditions. Thus, the hybrid is stable in sodium buffer up to ca. 50 °C; however, in potassium buffer, the telomeric DNA:RNA hybrid undergoes a transition to produce ss DNA and a DNA tetraplex thas is stable at > 50 °C. In contrast, the telomeric DNA:RNA hybrid duplex in sodium buffer melts at temperatures > 50 °C to produce ss RNA and ss DNA. The DNA:RNA hybrid duplex in potassium buffer is reformed upon cooling back to room temperature but some of the DNA remains "trapped" in a tetraplex structure. Possible implications of these observations with regard to telomere synthesis and the translocation process in the "inchworm model" will be discussed.

M-AM-D4

DIRECT MEASUREMENT OF THE FORCES BETWEEN COMPLEMENTARY STRANDS OF DNA WITH THE ATOMIC FORCE MICROSCOPE. ((G.U Lee, L.A. Chrisey, R.J. Colton)) Naval Research Laboratory, Code 6177, Washington, DC 20375-5342, U.S.A.

The AFM is an instrument possessing extreme force sensitivity (10^{-15} $N/\sqrt{Hz}$), a high immunity to ambient vibration and the capacity to control the separation between a probe and surface with 0.01 nm precision. We have used the AFM to study the forces between a probe and surface functionalized with molecular recognition systems. By controlling the density of molecules and area of the probe-surface contact we have demonstrated that it is possible to measure single molecular interactions between biotin and streptavidin (G. U Lee, D.A. Kidwell, R. J. Colton, *Langmuir* **10**, 354 (1994)). In this presentation we will discuss the interaction forces measured between complementary strands of DNA. Two types of forces have been identified: interchain forces associated with Watson-Crick base pairing between complementary strands of DNA and intrachain forces associated with the elasticity of single strands of DNA. Interchain forces manifest themselves as short-ranged adhesive forces of magnitude > 1.0 nN for a 20-mer in 0.1 N NaCl at room temperature. Intrachain forces are long-ranged adhesive forces that increase exponentially as the molecule is extended to its full length.

M-AM-D5

UNBINDING OF THE AVIDIN-BIOTIN COMPLEX ((E.-L. Florin, V.T. Moy, M. Ludwig, M. Rief and H. E. Gaub)) Department of Physics, Technische Universität München, 85748 Garching, Germany (Spon. by T.J. Feder)

Atomic force microscopy was applied to measure the unbinding force of individual avidin-biotin complexes. An examination of five avidin-biotin homologs revealed that the unbinding force quanta are proportional to the enthalpy change of the complex formation, but independent of changes in the free energy. In the avidin-iminobiotin system, though the equilibrium binding constant varied by 5 orders of magnitude over the pH range 4 to 10, the unbinding force quantum remained constant. These results are consistent with a model where the unbinding process is adiabatic and entropic changes transpire after unbinding. Based on the measured forces and binding energies, an effective rupture length of 9.5 ± 1 Å for the pair potential was calculated for all biotin-avidin combinations.

M-AM-D6

MODELING PROTEIN-LIGAND INTERACTIONS. ((R.W. Harrison I.V. Kourinov I.T. Weber)) Thomas Jefferson University, Philadelphia Pa 19107. (sponsored by Gregg B. Wells)

Molecular mechanics can be used to produce structural and energetic models for the interactions of proteins and ligands. The calculations must be performed in a physically consistent and numerically accurate manner for these models to be reliable. Our program AMMP has a fundamental improvement in accuracy by including all electrostatic and nonbonded terms without a cutoff radius. The cost of using all terms is controlled by spreading the cost of one expensive calculation over many calculations. It is also important to use an all-atom potential and a stable numerical integration scheme for molecular dynamics. The accuracy of the nonbonded terms is being improved by the use of non-point charges and polarization models for the atoms. Applications include the analysis of enzyme ligand interactions by modeling the complex and calculating the interaction energy. Correlation of the model structures and interaction energies with crystal structures and kinetic data such as Ki or kcat/Km indicates successful modeling for the examples of Human Glucokinase, HIV protease and Trypsin. Comparison of calculated interaction energies and observed binding constants shows when the internal energy or the entropy dominates the binding.

M-AM-D7

Pairwise Coupling: Deciphering Cooperativity Codes in Biological Macromolecules. Enrico Di Cera Dept Biochem & Mol Biophys, Washington Univ Med School, St. Louis, MO 63110.

Understanding the code for cooperative transitions in a biological macromolecule is a problem beset by many difficulties, either experimental and theoretical. When site-specific energetics are resolved experimentally, the various free energy levels defining the partition function of the system can be used to construct a number of thermodynamic cycles to assess 'pairwise coupling' between sites. This is done by choosing a particular pair of sites in its four possible ligated configurations, while keeping the configurations of the remaining sites fixed. The coupling free energy in the cycle is a measure of the communication between the sites constrained by the particular configuration of the rest of the macromolecule. The distribution of free energies of pairwise coupling reveals the exact mechanism of site-site communication and specifically whether the coupling is direct or mediated by other sites. The same strategy can be used in the analysis of mutational effects in proteins and nucleic acids. Free energies of pairwise coupling in this case reveal the communication patterns of domains specifically perturbed in a single or multiple site-specific fashion.

M-AM-D8

COMPUTER MODELING OF DIHYDROPYRIDINES BINDING IN THE PORE OF A SYNTHETIC Ca^{2+} CHANNEL.
((B.S. Zhorov and V.S. Ananthanarayanan)) Biochemistry Dept., McMaster Univ., Hamilton, Ont., Canada L8N 3Z5.

Grove et al. (*Proc.Natl.Acad.Sci. USA* **88**:6418, 1991) have demonstrated L-type Ca^{2+} channel activity of a synthetic 4-helix bundle having the sequence: DPWNVFDFLIVIGSIIDVILSE. The helices were linked to each other by the C-terminal nanopeptide template. Based on our earlier proposal on Ca^{2+} role in ligand-receptor recognition, we sought to obtain the optimal conformations of the above calcium channel protein and locate the binding sites for Ca^{2+} and for the dihydropyridine (DHP) ligand. We used Monte Carlo with energy minimization method. Eight Ca^{2+} ions were added to neutralize negative charges of the protein. Six of them were chelated by the 12 acidic residues in the pore (Glu^{22}, Asp^{17} and Asp^{7}). The ligand fit snugly in the pore with the flattened-boat DHP ring orthogonal to the pseudoaxial 4-aryl group at the "bowsprit". The substituents at the starboard and port sides were extended in extra- and intracellular directions, respectively. The polar groups in the starboard and bowsprit along with two Asp^{17} residues were involved in Ca^{2+} binding. The port polar group was situated proximal to the ring of four Ile^{12}. This arrangement is seen to facilitate the passage of Ca^{2+} via the ring of Ile^{12}. This would explain the channel activator's action. In contrast, channel blockers have a hydrophobic moiety at the port side and this increases the barrier to Ca^{2+} passage. (Sponsored by NSERC and CHF, Canada).

M-AM-D9

A SAMPLING PROBLEM IN MOLECULAR DYNAMICS SIMULATIONS OF MACROMOLECULES

J. B. Clarage, T. D. Romo, B. K. Andrews, B. M. Pettitt†
G. N. Phillips Jr.,
Keck Center for Computational Biology
Dept. of Biochemistry and Cell Biology
Rice Univ., Houston, TX 77251
† Dept. of Chemistry, Univ. of Houston,
Houston, TX 77204-5641
(email: clarage@rice.edu, WWW http://helix.rice.edu/~clarage/science)

Correlations in low frequency atomic displacements predicted by molecular dynamics simulations on the order of one nanosecond are under-sampled for the timescales currently accessible by the technique. This is shown with three different representations of the fluctuations in a macromolecule: the reciprocal space of crystallography using diffuse X-ray scattering data; real 3-dimensional Cartesian space using covariance matrices of the atomic displacements; and the 3N-dimensional configuration space of the protein, using dimensionally reduced projections to visualize the extent to which phase space is sampled.

(This work supported by NIH, NSF, The W.M. Keck Center for Computational Biology, and the Robert A. Welch Foundation.)

ELECTRON-PROTON TRANSFER PROTEINS

M-AM-E1

RUBREDOXIN: UNDERSTANDING PROTEIN AND SOLVENT CONTRIBUTIONS TO ELECTRON TRANSFER PROPERTIES BY MOLECULAR DYNAMICS SIMULATIONS ((R. B. Yelle and T. Ichiye)) Department of Biochemistry/Biophysics, Washington State University, Pullman, WA 99164-4660.

Molecular dynamics simulations of the oxidized and reduced forms of *Clostridium pasteurianum* rubredoxin, an iron-sulfur protein, have been carried out. The simulations show good agreement with the oxidized crystal structure, with root mean-square backbone deviations of 1.06 and 1.42 Å, respectively. An increase in the solvation of the iron-sulfur site is seen, as has been seen in NMR studies of cytochrome *c*, by J. Wand and co-workers. The role of these and other non-linear effects in lowering activation energies to electron transfer relative to those predicted from Marcus theory are discussed.

M-AM-E2

UNDERSTANDING THE CYTOCHROME *C* OXIDASE PROTON PUMP: THE ENERGETICS OF REDOX LINKAGE. ((S. M. Musser)) Arthur Amos Noyes Laboratory of Chemical Physics, California Institute of Technology, Pasadena, CA 91125. (Spon. by NIH)

The cytochrome *c* oxidase complex (CcO) catalyzes the four-electron reduction of dioxygen to water using electrons from ferrocytochrome *c*. A portion of the redox free energy released in this highly exergonic process is utilized to drive the translocation of protons across a transmembrane electrochemical gradient. It is clear that redox energy must drive the endergonic proton pumping reactions, but few attempts have been made to explain the stepwise transfer of energy in the context of proposed protein conformational changes. A model which seeks to clarify the energetics of CcO's proton pumping function and which illustrates the importance of electron and proton gating to prevent the occurence of the more exergonic electron leak and proton slip reactions will be presented. In this model, the redox energy of the CcO-membrane system is formulated in terms of a multidimensional energy surface projected into two dimensions: a nuclear coordinate associated with electron transfer (NCET); and, a nuclear coordinate which describes conformational changes of the proton pump (NCPP). Within this construct, efficient proton pumping is achieved only when electron and proton gating mechanisms kinetically enhance the desired reactions over the more exergonic uncoupling reactions. This model also provides an understanding of how a transmembrane electrochemical gradient affects the efficiency of the proton pumping process. Specifically, electron leak and proton slip reactions become more probable due to the greater energy barriers which develop for the desired reactions in the presence of a transmembrane potential.

M-AM-E3

AN EXPERIMENTAL TEST OF A LIGAND SWITCHING MECHANISM FOR CYTOCHROME *c* OXIDASE. ((J. Hosler[1], J. Fetter[1], D. Mitchell[3], M. Pressler[2], J. Alben[4], R. Gennis[3], G. Babcock[2] and S. Ferguson-Miller[1])) Depts. of [1]Biochem. and [2]Chem., Michigan State U., E. Lansing, MI 48824; [3]Dept. of Biochem., U. of Illinois, Urbana, IL, 61801; [4]Dept. Med. Biochem., Ohio State U., Columbus, OH 43210.

A recurring theme in postulated mechanisms of proton pumping by cytochrome oxidase is ligand exchange at one of the redox active metals during oxygen reduction. A detailed proton pumping scheme described by Rousseau *et al.* (1993, *J. Bioenerg. Biomemb. 25:* 165) proposes the exchange of Y422 for H419 as the proximal ligand of heme a_3. To test this, Y422 was altered to A, F, and H. All three mutant oxidases transfer electrons at ~ 40% of the wild-type rate. Y422A and F were reconstituted into phospholipid vesicles and found to pump protons with the same efficiency as wild-type. A ligand switching mechanism involving Y422 is thus not tenable. Analysis by optical, RR, EPR and FTIR spectroscopies shows that each of the three alterations of Y422 causes unique changes in the structure of the heme a_3-Cu_B center, while heme *a* appears unaffected. The Y422H spectra suggest multiple orientations of heme a_3 and changes in the ligand environment of Cu_B. Y422F favors the beta forms of CO-ligated heme a_3 and Cu_B, while Y422A shows heme a_3 RR vibrational modes reminiscent of mammalian oxidase. These results indicate that the structure of the heme a_3-Cu_B center can be affected by changes on the proximal side of heme a_3, even while enzyme activity is retained.

M-AM-E4

THE PATHWAY OF CO BINDING TO CYTOCHROME c OXIDASE. CAN THE GATEWAY BE CLOSED? **((Bruce C. Hill)) Dept. Biochem., Queen's U., Kingston, ON, Canada K7L 3N6.**

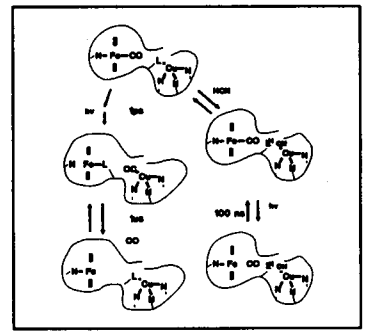

Addition of cyanide to cytochrome oxidase-CO reduces the apparent photosensitivity of the Fe-CO bond. This effect is not seen with azide, or when cyanide is added to ferromyoglobin-CO. It is proposed that cyanide binds to Cu_B, restricts passage of CO out of the protein, and favors geminate recombination of CO and ferrocytochrome a_3, thereby lowering the apparent quantum yield for CO photolysis. The apparent K_D of cyanide for Cu_B is 15.4 mM. These data support a direct role for Cu_B in ligand binding by cytochrome c oxidase. (Supported by NSERC Canada).

M-AM-E5

FLUORESCENCE QUENCHING OF 9-ANTHRACENEPROPIONYL CARDIOLIPIN BY CYTOCHROME *c* OXIDASE AS A MEASURE OF CARDIOLIPIN BINDING AFFINITY. ((M. Panda and N. C. Robinson)) Dept. Biochemistry, Univ. Texas Health Sci. Cntr, San Antonio, TX 78284. (Spon. by S. A. Khan)

Bovine heart cytochrome c oxidase(COX) requires 2 mol of tightly bound cardiolipin (CL) in order to maintain full electron transport activity (Robinson et al. (1990) *Biochemistry*, 29 8962). Here we have used quenching of the fluorescent CL analogue, 9-anthracenepropionyl cardiolipin (APCL), by COX was used to estimate the binding affinity of CL to COX. APCL is an excellent probe of the CL binding site because it is as effective as natural CL in restoring full electron transport activity to CL-depleted COX. APCL is strongly fluorescent when it is dissolved in detergent micelles, but is quenched by the heme centers of COX when it is bound to oxidase. From the dependence of total quenching as a function of added [APCL], non-specific and specific binding constants were evaluated. A value of $K_{d,app}$ = 1.6 μM was obtained for the binding constant of the 2 CL specific sites. This value is only two times greater than that determined indirectly from activity studies and much lower that determined from ^{14}[C]-Acetyl-CL binding experiments (Robinson et al., 1990). Therefore, we believe that the binding constant for APCL accurately reflects the intrinsic binding constant for CL.
Supported by research funds from NIGMS 24795.

M-AM-E6

EFFECT OF AMPHIPHILIC ENVIRONMENT SURROUNDING CYTOCHROME *c* OXIDASE UPON STEADY STATE REDUCTION OF CYTOCHROME *a* . ((J. Ortega-Lopez and N. C. Robinson)) Department of Biochemistry, Univ. Texas Health Sci. Center., San Antonio, TX 78284.

Reduction levels of cytochrome *c* and cytochrome *a* were measured by multiwavelength visible spectroscopy under steady state turnover at low ionic strength, pH 7.9, using ascorbate as the primary electron donor. Reduction levels of both cytochrome *c* and cytochrome *a* were influenced by the concentration of TMPD (N,N,N',N'-tetramethyl-p-phenylenediamine) and the type of detergent bound to cytochrome *c* oxidase. In dodecyl maltoside, a detergent that supports high activity, reduction of cytochrome *c* and cytochrome *a* were strongly dependent upon the TMPD concentration and only 50% and 70%, respectively, were reduced even at 2 mM TMPD. However, in Triton X-100, a detergent that only supports low activity, full reduction of both cytochrome *c* and cytochrome *a* were achieved even with a low TMPD concentration, i.e. 0.5 mM. Other detergents gave intermediate results. In general, the percent reduction of cytochrome *c* and cytochrome *a* was inversely correlated with cytochrome c oxidase enzyme activity . These results suggest that at least half of the second phase of the steady-state cytochrome *c* oxidase kinetics is due to the increased reduction of cytochrome *a* by unbound cytochrome *c*.
Research supported by NIGMS 24795.

M-AM-E7

ENERGY COUPLING MEDIATED BY SUBUNIT III OF CYTOCHROME C OXIDASE **(S. Wu, R. Moreno-Sanchez and H. Rottenberg) pathology, Hahnemann University, Philadelphia, PA 19102.**

Subunit III is conserved in all H^+-pumping terminal oxidases but its function is unknown. H^+-pumping in site-directed mutants of glu98 of subunit III of the P. Denitrificans cytochrome c oxidase (COX) is not impaired (Haltia et al EMBO J. 10, 2015, 1991). We have studied the efficiency of oxidative phosphorylation and $\Delta\tilde{\mu}$ generation by COX in starved cells and membrane vesicles of these mutants. The mutants glu98ala and glu98gln have significantly lower efficiency than wt in oxidative phosphorylation with ascorbate/TMPD or succinate while the rates of electron transport are similar or faster than wt. The magnitude of $\Delta\tilde{\mu}$ which is generated by COX, quinol oxidase, or ATP synthase is comparable in mutants and wt. Oxidative phosphorylation by the quinol oxidase is also not impaired in these mutants. The glu98asp mutant is only marginally affected. These results may be interpreted as an indication for participation of glu98 of subunit III of COX in direct coupling to ATP synthase.

M-AM-E8

PHOTOREDUCTION OF CYTOCHROME C AND OTHER HEME PROTEINS BY NEW NITROBENZENE DERIVATIVES. ((T.J. DiMagno, M.H.B. Stowell and S.I. Chan)) California Institute of Technology, Pasadena, CA 91104.

A series of tri-substituted nitrobenzene derivatives have been synthesized for use as photoreductants of cytochrome *c* and other heme proteins. These nitrobenzene derivatives exhibit many desirable characteristics suitable for the photoreduction of protein systems that current photoreductants lack. First, the photoreductant undergoes irreversible chemistry following electron transfer so that no back electron transfer occurs. Second, the absorption profile of these photoreductants has no absorbance > 410 nm so that no spectral overlap with the protein chromophores occurs. Furthermore, the absorption spectrum of these photoreductants can be tuned by synthetically modifying the various substituents on the nitrobenzene framework. Finally, the binding properties of the photoreductant with protein can be altered by adding appropriate charged substituents on the parent nitrobenzene. This allows the photoreductant to be engineered to optimize electron transfer to a given protein with a known pI. The observed photoreduction of cytochrome *c*, k_{obs}, ranged from 300 s^{-1} to 36,000 s^{-1} for these derivatives. The effects of pH, ionic strength, and various substituents on the photoreduction of cytochrome *c* are reported. A kinetic model for this bimolecular reaction is described to provide the inherent electron transfer rate constant, k_{et}.

M-AM-E9

AN INVESTIGATION OF FUNCTIONAL SIGNIFICANCE FOR THE CONSERVED NONPLANAR HEME DISTORTION IN CYTOCHROMES *C*

((J. D. Hobbs[1] and J. A. Shelnutt[1,2])) [1]*Fuel Science Department, Sandia National Laboratories, Albuquerque, NM 87185-0710.* [2]*Department of Chemistry, University of New Mexico, Albuquerque, NM 87131.*

Nonplanar macrocyclic conformations have long been postulated to play an important role in the biological function of tetrapyrrole containing proteins. A recent examination [Hobbs & Shelnutt, *J. Protein Chem.* in press] of high-resolution (≦2.0 Å) X-ray crystal structures of *c*-type cytochromes isolated from eight species reveals the presence of a conserved, asymmetric nonplanar distortion of the heme that is induced through the covalent linkages between the heme peripheral substituents and amino acid residues of the protein. Further, resonance Raman studies [Anderson, et al. *J. Am. Chem. Soc*, 1993, *115*, 12346] of metallooctaethylporphyrins and meso-nitrooctaethylporphyrins have been used to estimate the energy required by the protein to distort porphyrins possessing large metal core sizes from their preferred planar geometry. Herein, we present results from molecular dynamics calculations for yeast iso-1-cytochrome *c*, starting from the crystal coordinates. These calculations have been employed to examine the role of porphyrin nonplanarity in protein tertiary structural changes occurring between the ferric and ferrous species.

Supported by U.S. DOE Contract DE-AC04-94AL85000 and Associated Western Universities Fellowships (JDH)).

M-AM-E10

MECHANICAL CONTROL OF REDOX ENTHALPY CHANGE FOR ELECTRON TRANSFER TO PROTEIN SITES. ((A.S. Brill))

Department of Physics, University of Virginia, Charlottesville, VA 22901.

The geometry of free complexes of copper and iron depends upon the valence of the metal ion. When such a site is part of a protein, the geometries of the oxidized (A) and reduced (D) forms are affected by the protein structure. The degree of constraint which is imposed depends upon the local stiffness. The elastic contribution to the enthalpy change accompanying electron transfer to the site is

$\Delta H_{elastic} = [k_P k_D/2(k_P + k_D)](q_P^2 - q_D^2) - [k_P k_A/2(k_P + k_A)]q_P^2$ with $q_A = 0$.

k_P is the stiffness of the site on the apoprotein, k_A of the oxidized and k_D of the reduced states in the free metal complexes, and the q_i are the minima of the associated harmonic potentials. To illustrate the geometrical effect, we take $k_A = k_D = k$ and find $\Delta H_{elastic} = [k_P k/(k_P + k)]q_D(0.5q_D - q_P)$. The role of the protein in setting q_P is seen to be critical. The dependence of the sign and magnitude of $\Delta H_{elastic}$ upon $(0.5q_D - q_P)$ will be demonstated. For the cupric site in azurin, for which the relevant mode is torsional, the control sensitivity is surprisingly large: $d\Delta H_{elastic}/dq_P$ is about -2kcal/mol per degree increase in the out-of-planarity angle.

MUSCLE MECHANICS AND ULTRASTRUCTURE

M-AM-F1

OSCILLATIONS IN THE ORIENTATION OF ACETAMIDOTETRAMETHYL-RHODAMINE (ATR) PROBES ON MYOSIN REGULATORY LIGHT CHAIN (RLC) CAUSED BY SINUSOIDAL LENGTH CHANGES IN SKINNED MUSCLE FIBERS

((Seth C. Hopkins*, Le Phan*, Malcolm Irving+ and Yale E. Goldman*, +Randall Inst., King's Coll. London and *Pennsylvania Muscle Inst., Univ. of PA))

In actively contracting muscle fibers, quick length changes (ΔL) elicit small changes (ΔΘ) in the orientation of the light chain region of myosin (Allen et al. *Biophys. J.* 66: A234, 1994). ΔΘ/ΔL has the opposite sign in rigor. We investigated the time course of this change in ΔΘ/ΔL by imposing 2.6 nm / ½ sarcomere, 500 Hz sinusoidal length changes during activation of *psoas* muscle fibers from rigor by photolysis of caged ATP (~30 μM free Ca^{2+}, ionic strength, 200 mM, 12 °C). Gizzard RLC, labeled at Cys108 with pure 6-isomer of ATR (Corrie & Craik, *J. Chem. Soc., Perkin Trans.* 1:2967, 1994), was exchanged into single fibers. The fluorescence polarization ratio, $Q_\perp$, was measured as described by Allen et al. In rigor, $Q_\perp$ oscillated in phase with the imposed length change ($\Delta Q_\perp/\Delta L$ in Fig. is positive). Release of ATP caused a prompt decrease in $Q_\perp$ and a decrease then increase in tension, as reported before. $\Delta Q_\perp/\Delta L$ became negative, indicating that the $Q_\perp$ oscillations went out of phase with ΔL. $\Delta Q_\perp/\Delta L$ changed more slowly than $Q_\perp$ but before tension developed suggesting that ΔΘ/ΔL for pre-force bridges is like that for force-generating ones. We thank J. Kendrick-Jones, C. Sabido-David, D.R. Trentham and B. Brandmeier for preparation and characterization of labelled RLC. Supported by NIH grant AM26846, the MDA and the Wellcome Trust, UK.

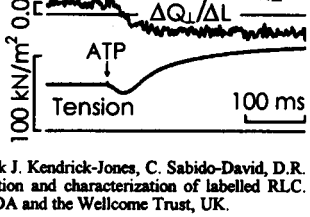

M-AM-F2

SPATIAL DIMENSIONS OF ATTACHED CROSSBRIDGES IN THE FILAMENT LATTICE OF RELAXED, ACTIVATED AND RIGOR MUSCLE

((B. Brenner*, S. Xu+, J.M. Chalovich# and L.C. Yu+)) *Medical School Hannover, Germany; #E.Carolina Med. School, NC; +NIH, Bethesda, MD.

In characterizing structural properties of crossbridges during muscle contraction, not only the knowledge of the crystal structures of actin and myosin is essential, but also the three dimensional space confined by the thick and the thin filaments available for actomyosin interaction. By studying the resistance to osmotic compression in skinned rabbit psoas fibers, we reported earlier that when a cross-bridge attaches to actin, it generates radial force capable of changing the separations between the filaments. Furthermore, the surface to surface distance between filaments for which the attached cross-bridges are **undistorted** in the lateral direction is different for different cross-bridge states, indicating distinct structures of the attached cross-bridges (Brenner & Yu, J. Physiol., 1991; Xu, et al., J. Physiol., 1993). In the present study, we found that at ionic strength of 80 mM, the characteristic surface-to-surface distance for (i) the preforce, weakly bound state, (ii) the force generating state and (iii) the rigor state are at 375, 353, 390Å respectively. One cannot distinguish whether the results are due to differences in the shape of the myosin head and/or its mode of attachment to actin. Nevertheless, these characteristic filament distances define spatial constraints that modelling of the attached cross-bridges in these states must satisfy; i.e. our results provide an evelope for fitting the attached crossbridges in the filament lattice.

Supported by NATO collaborative research grant #930448.

M-AM-F3

2D-X-RAY DIFFRACTION STUDIES ON THE EFFECT OF CALCIUM ON WEAK CROSS-BRIDGE BINDING TO ACTIN IN THE PRESENCE OF ATPγS.

((T.Kraft*, S.Xu*, B.Brenner§, L.C.Yu+)) *NIH, NIAMS, Bethesda, MD; §Medical School, Hannover, FRG.

We previously proposed that isometric force results from a structural change when an attached crossbridge changes from the weakly bound configuration to its strongly attached form. In earlier studies we had characterized the structure of the weakly bound crossbridge only in the absence of Ca^{++} (relaxing conditions). We now examined whether activation of the thin filament (e.g. by Ca^{++}) affects the mode of weak crossbridge binding to actin. To avoid active crossbridge cycling when raising Ca^{++} we used ATPγS as an ATP analog of which we had shown that it is an analog of weak binding crossbridge states (Kraft et al., PNAS, 1991). In this previous study we also found that although actin affinity is only little affected by Ca^{++}, actin binding kinetics are almost 100-fold slowed down, suggesting that the mode of weak crossbridge binding might be different in the presence of Ca^{++}. Since in fiber bundles we found effects of nucleotide depletion due to slow hydrolysis of ATPγS, it was essential for this study to use single fibers of which we mounted up to 30 simultaneously in the setup to obtain sufficient intensities in the diffraction patterns. We found that equatorial intensities in the presence of ATPγS are little affected by Ca^{++}, and at both high and low Ca^{++} myosin layer lines appear similar to those of fibers relaxed in the presence of ATP. Also, no obvious enhancement of the first actin layer line is detectable at high Ca^{++}, all findings pointing to no large changes in the mode of weak crossbridge binding to actin upon activation.

M-AM-F4

FAST 2-D X-RAY DIFFRACTION STUDIES OF CONTRACTING BONY FISH MUSCLE: TOWARDS 'MUSCLE - THE MOVIE'

((J.J. Harford, L. Hudson, R. Denny and J.M. Squire)) Biophysics Section, Blackett Laboratory, Imperial College, London SW7 2BZ, UK.

Low-angle 2-D X-ray diffraction patterns from bony fish muscle (Harford et al (1994) J.Mol.Biol. 239, 500-512) contain sufficient information to allow modelling using the known myosin head shape. A series of such 2-D diffraction patterns has been recorded at 5 ms time intervals during a typical tetanic contraction of plaice fin muscle (Harford & Squire (1992) Biophys.J. 63, 387-396). The problem of separating the well-defined Bragg peaks from the asymmetric, smooth background to give reliable intensities (J(hkl)) for the Bragg peaks has been tackled using new software developed as part of the BBSRC Collaborative Computing Project in Fibre Diffraction (CCP13). A new program has also been written to read in the stripped I(hkl) values and the head shape and to search over parameter space (head orientation, tilt, rotation, radius etc) to give the best R-factor or correlation coefficient values between observed and calculated intensities. Refinement procedures utilising downhill simplex, Powell's method or simulated annealing routines are being used to optimise the modelling. Following this, refinement can be continued by combining model phases and observed amplitudes. The resulting relaxed fish muscle structure can be used as part of a boot-strapping exercise to determine the fish muscle unit cell contents as force is gradually generated through the tetanic contraction. This will provide a time sequence of images from which to compile 'Muscle - The Movie'. Included in this will be modelling of the actin filament structure during activation, including both the tropomyosin shift and actin sub-domain movements (Squire et al (1994) Biophys. Chem. 50, 87-96). WORK SUPPORTED BY BBSRC & MRC.

M-AM-F5

TOMOGRAPHIC 3-D IMAGE RECONSTRUCTION OF IFM IN RIGOR AND IN THE PRESENCE OF AMPPNP. ((H. Schmitz, H. Winkler[1], M. C.. Reedy[1], M. K. Reedy[1], R. T. Tregear[2] and K. A. Taylor[1])) [1]Dept. of Cell Biology, Duke Univ. Medical Center, Durham, NC 27710, [2]MRC Lab. of Molec. Biol., Hills Road, Cambridge CB2 2QH, UK.

Even highly ordered insect flight muscle (IFM) possesses substantial disorder, especially during contraction or in states produced using non-hydrolyzable ATP analogues such as AMPPNP. In order to understand the interplay between structure, tension and stiffness, we have embarked on tomographic 3-D imaging of IFM in these disordered states as well as in rigor. Tomography produces a 3-D image without averaging but the image appears much noisier because of intrinsic structural variations as well as preparative inhomogeneities. The reconstructions are obtained by combining up to 40 images spread over a tilt range of ±75°. Tomograms of rigor IFM reveal double headed lead and single headed rear crossbridges as described previously. Tomograms of IFM treated with aqueous AMPPNP at 22°C contain predominately single headed crossbridges. When the tomogram itself is averaged over the crystallographic unit cell, the 3-D image is nearly identical to that obtained by oblique section reconstruction which shows only paired lead bridges every 38.7 nm period angled similarly to their rigor counterpart. However, the nonaveraged tomogram shows additional crossbridge forms that have no correspondence with either the lead or rear bridge motifs seen in rigor muscle. Some of these occur in antirigor angles; others are located in the interdoublet gap outside of the actin target zones defined for rigor. These observations suggest that the rear bridges of rigor have redistributed on treatment with AMPPNP which could explain the maintenance of rigor stiffness despite loss of 70% of rigor tension. Supported by NIH grants GM-30598 and AR-14317.

M-AM-F6

STRUCTURE OF IFM IN THE PRESENCE OF AMPPNP BY OBLIQUE SECTION 3-D IMAGE RECONSTRUCTION. ((H. Winkler[1], M. C.. Reedy[1], M. K. Reedy[1], R. T. Tregear[2] and K. A. Taylor[1])) [1]Dept. of Cell Biology, Duke Univ. Medical Center, Durham, NC 27710, [2]MRC Lab. of Molec. Biol., Hills Road, Cambridge CB2 2QH, UK.

Treatment of insect flight muscle (IFM) in rigor with aqueous AMPPNP at 22°C causes a 70% drop in tension with little change in stiffness. Electron micrographs suggest a change in the structure of the crossbridges near the thick filament. We have examined the structure of this state using oblique section 3-D reconstruction (OSR). Data from both transverse and longitudinal oblique sections were combined in space group P1 to produce an averaged 3-D image with isotropic resolution. The structure of IFM in rigor obtained by OSR revealed periodic double chevrons comprising two-headed lead bridges and one-headed rear bridges. The averaged 3-D image from IFM in AMPPNP contains only one crossbridge pair per 39 nm actin repeat, forming a single chevron resembling rigor's lead bridge pair in 45° angle and in position with respect to troponin. At the position where rear bridges appear in rigor, this OSR shows no comparable feature. A pronounced density on the thin filaments is located midway between consecutive chevrons, where troponin has been observed in rigor by antibody labeling and by 3-D reconstruction. The single-chevron bridges in AMPPNP are smaller and of lower density than rigor lead bridges, indicating less order and suggesting that many crossbridges are single-headed. The apparent loss of rear bridges might explain the drop in tension but not the unchanged stiffness. Stiffness could stay unchanged if the rear bridges have redistributed, reattaching in a more disordered arrangement at positions of lower average strain. Supported by NIH GM-30598 & AR-14317.

M-AM-F7

FLUORESCENCE POLARIZATION CHANGES AND MECHANICAL EVENTS FOLLOWING PHOTOLYSIS OF CAGED ATP IN RABBIT *PSOAS* MUSCLE FIBERS LABELED AT SH-1 WITH ISOMERS OF ACETAMIDOTETRAMETHYLRHODAMINE (ATR). ((C.L. Berger[1], J.S. Craik*, D.R. Trentham*, J.E.T. Corrie*, and Y.E. Goldman. Pennsylvania Muscle Institute, University of Pennsylvania, Philadelphia, PA 19104 and *National Institute for Medical Research, Mill Hill, London NW7 1AA, U.K. [1]Present address: Department of Molecular Physiology & Biophysics, University of Vermont, Burlington, VT 05405))

We have previously shown that following photolysis of caged ATP in single rabbit *psoas* muscle fibers, labeled at SH-1 (Cys-707 of myosin heavy chain) with either the 5- or 6-isomer of ATR, fluorescence polarization ratios, $Q_t = (I_t - {}_\perp I_\perp)/(I_t + {}_\perp I_\perp)$ and $Q_\perp = ({}_\perp I_\perp - I_\perp)/({}_\perp I_\perp + I_\perp)$, change markedly before active force generation (Berger et al., (1994) *Biophys. J.* 66:A234). In order to determine whether the changes of Q_t and $Q_\perp$ accompany the detachment of rigor cross-bridges, we examined the time course of tension, Q_t and $Q_\perp$ at various ATP concentrations following photolysis. Cross-bridge detachment (R→D in Fig. estimated from fitting a simple kinetic model to the tension traces (scheme IV of Dantzig et al., (1991) *J. Physiol.* 432:639)) was slower than the changes of Q_t and $Q_\perp$. Fluorescence polarization was almost constant during reattachment and force generation (D→A in Fig.). These results are consistent with motions at SH-1 on the communication pathway between the nucleotide and actin binding sites of myosin. Supported by the NIH (AR26846), MDA & MRC.

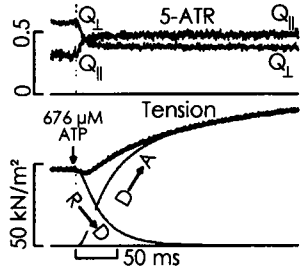

M-AM-F8

PHOSPHORESCENTLY LABELED GIZZARD REGULATORY LIGHT CHAINS REVEAL DIFFERENCES IN MYOSIN ROTATIONAL DYNAMICS BETWEEN SCALLOP AND RABBIT MUSCLE.
((Sampath Ramachandran and David D. Thomas)) U. of Minnesota, Minneapolis, MN 55455. (Spon. by David Levitt)

Time-resolved phosphorescence anisotropy (TPA) has been used to probe the rotational dynamics of chicken gizzard regulatory light chain (GRLC) incorporated into scallop adductor and rabbit psoas myofibrils. GRLC was site-specifically labeled at Cys 108 with phosphorescent probes and introduced with full restoration of function into the myofibrils depleted in native regulatory light chains. In rigor, anisotropy showed little decay, indicating a nearly immobile probe. Both systems showed increased amplitude of microsecond rotation upon addition of ATP (relaxation) as evidenced by lower anisotropy values. Activation of relaxed myofibrils with Ca^{+2} causes a substantial change in the decay. However, **the addition of Ca^{+2} to relaxed myofibrils has opposite effects in these two systems:** the amplitude of microsecond rotation decreases in scallop but increases in rabbit. This indicates **differ-ences in the molecular dynamics of the light chain binding region in response to activation,** probably due to the different activation mechanisms in the two muscle types.

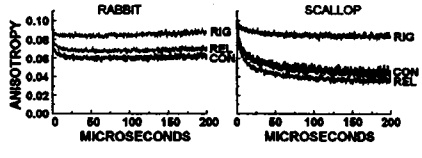

ELECTROSTATIC FORCES IN MACROMOLECULAR FUNCTION

M-AM-SymII-1

Macroscopic Treatments of Electrostatic Free Energies: Applications to Protein and Nucleic Acid Structure and Function

Dr. Barry Honig, Columbia University, Department of Biochemistry and Molecular Biophysics, 630 West 168th Street, N.Y., N.Y.10032

The application of macroscopic solvent models to problems associated with protein and nucleic acid structure and function will be discussed. Electrostatic phenomena are treated with the Poisson-Boltzmann (PB) equation. The physical basis of the PB equation will be discussed and recent development in its numerical solution will be summarized. A number of recent applications will be described. These will range from qualitative insights derived from displays of electrostatic potentials maps around proteins using the GRASP program to quantitative calculations on problems such as pH effects on protein stability, salt effects on protein/nucleic acid interactions, and the free energy balance in protein folding.

M-AM-SymII-2

ELECTROSTATICS MEDIATES THE BINDING OF SRC AND MARCKS TO MEMBRANES. ((S. McLaughlin, R. Peitzsch, C. Buser, J. Kim)) Dept. Physiology & Biophysics, SUNY, Stony Brook, NY 11794.

We used the Poisson-Boltzmann equation to calculate the electrostatic potential in the aqueous phase adjacent to realistic molecular models of phospholipid bilayers. When the membranes contain > 25% acidic lipid, the calculations agree well with predictions of Gouy-Chapman theory, which describes adequately the experimental results obtained with phospholipid bilayers by several laboratories. We also examined how a combination of hydrophobic and electrostatic interactions direct the membrane binding of several proteins involved in signal transduction. The N-terminal myristate (14 C acyl chain) of Src and MARCKS inserts into the hydrocarbon interior of the membrane, and a cluster of basic amino acids interacts with acidic lipids. The individual hydrophobic or electrostatic interactions are too weak to attach these proteins firmly to membranes, but a simple model predicts correctly that the individual binding energies add (partition coefficients multiply). The cluster of basic residues on MARCKS contains the only residues phosphorylated by PKC: phosphorylation reduces the net positive charge of the cluster, producing translocation of MARCKS (and Src) from the plasma membrane to cytoplasm in living cells and from phospholipid vesicles to solution *in vitro*. A Gouy-Chapman/mass action model accounts for this "electrostatic switching" mechanism.

M-AM-SymII-3

INTERACTION OF PROFILIN AND MYOSIN-I WITH MEMBRANE PHOSPHOLIPIDS. (Thomas D. Pollard, Department of Cell Biology and Anatomy, Johns Hopkins Medical School, Baltimore, MD 21205)

The actin binding proteins profilin and myosin-I also interact with phospholipid head groups in biological membranes. Profilin binds to small clusters of phosphatidylinositol 4-phosphate and 4,5-bisphosphate. The dissociation equilibrium constant is about 1μM. Two regions on the surface of profilin have positive electrostatic surface potentials and are candidate binding sites for the negatively charged lipid head groups. In surface plasmon resonance experiments with lipid micelles or vesicle binding to profilin immobilized on dextran coated sensor chips both association and dissociation are slow: k_+ is $10^{-2}\mu M^{-1}\,s^{-1}$ and k_- is $10^{-2}s^{-1}$. By binding to PIP_2 profilin inhibits the production of the second messengers IP_3 and DAG by phospholipase Cγ1. Tyrosine phosphorylation of the phospholipase by the EGF receptor overcomes this inhibition. This negative regulation by profilin allows receptor activation to control the production of IP_3 and DAG. On the other hand, cell stimulation of the receptor may release profilin to stimulate actin assembly. Myosin-I binds acidic phospholipids, but is less discriminating, since it interacts with phosphatidylserine, phosphatidylinositol, PIP_2 or phosphatidic acid. For a neutral lipid bilayer with physiological concentration of phosphatidylserine, the dissociation constant for myosin-I is <0.1μM. The lipid binding site of myosin-I is a domain of about 250 residues with a high net positive charge located in the proximal part of the tail. Binding to an immobilized lipid bilayer is strong enough for myosin-I to support the gliding of actin filaments. The association of the various myosin-I isozymes with different cellular membranes suggests that interactions with membrane proteins provide specificity not found in the lipid interactions. (Supported by NIGMS)

M-AM-SymII-4

STRUCTURES OF DNA POLYMERASE PROCESSIVITY FACTORS. ((J. Kuriyan)) Rockefeller Univ.

CHANNEL ELECTROPHYSIOLOGY

M-AM-G1

STIMULATION OF SINGLE L-TYPE CALCIUM CHANNELS IN RAT PITUITARY GH3 CELLS BY THYROTROPIN-RELEASING HORMONE. ((M. Mantegazza, C. Fasolato, J. Hescheler and D. Pietrobon) Dept. Exp. Biomed. Sci., C.N.R. Center of Mitoch. Physiol., Univ. of Padova, 35131 Padova.

Hormonal stimulation of voltage-dependent Ca^{2+} channels in pituitary cells is thought to contribute to the sustained phase of Ca^{2+} entry and secretion induced by secretion-stimulating hormones and has been suggested as a mechanism for refilling the Ca^{2+} stores. Using the cell-attached patch-clamp technique, we studied the stimulation of single Ca^{2+} channels by thyrotropin-releasing hormone (TRH) in rat GH_3 cells. We show that TRH applied from the bath switched the activity of single L-type Ca^{2+} channels from a gating mode with very low open probability (p_O) to a gating mode with slightly smaller conductance but ten times higher p_O. Interconversions between these two gating modes were observed also in basal conditions, where the equilibrium was largely shifted towards the low-p_O mode. TRH applied from the pipette had no effect, indicating the involvement of a cytosolic compound in the stimulatory pathway. We show that TRH does not potentiate all the L-type Ca^{2+} channels in a given membrane patch and that GH_3 cells coexpress two functionally different L-type Ca^{2+} channels, suggesting selective potentiation of only one channel subtype. Our results uncover the biophysical mechanism of hormonal stimulation of voltage-dependent Ca^{2+} channels in GH_3 cells, and are consistent with differential modulation of different subtypes of dihydropyridine-sensitive Ca^{2+} channels.

M-AM-G2

"LOCAL" VS. "DISTANT" EFFECTS OF ISOPRENALINE ON CARDIAC L-TYPE Ca^{2+} CURRENT. ((R. Fischmeister and J. Jurevicius)) INSERM CJF 92-11, Univ. Paris-Sud, Fac. Pharmacie, 92296 Châtenay-Malabry, France.

β-adrenergic stimulation of cardiac L-type Ca^{2+} current (I_{Ca}) is the final step of a sequence of events that includes activation of the β-receptor, activation of G_s proteins, activation of adenylyl cyclase, accumulation of cAMP, activation of cAMP-dependent protein kinase, and phosphorylation of Ca^{2+} channels or a regulatory protein. Our aim here was to investigate the role of subcellular compartmentation in the progress of these sequential events. We used a double-barrelled perfusion method described by us at this meeting to measure "local" and "distant" effects of isoprenaline (ISO), a β-adrenergic agonist, on I_{Ca} measured in frog ventricular cells. When ≈half of the cell length was exposed to a 0Ca-solution (nominal), basal I_{Ca} was reduced by ≈50%. In 6 different cells, successively increasing concentrations of ISO (1 nM-10 μM) were then added to the part of the cell exposed to 0Ca. A progressive increase in I_{Ca} developped at > 10 nM ISO which was due to the stimulation of the Ca channels present in the remote part of the cell not exposed to ISO but exposed to Ca. This "distant" effect of ISO was compared to the "local" effect of ISO obtained when adding the drug to the other part of the cell. At saturating concentrations (3-10 μM), the distant effect of ISO on I_{Ca} was only 30-50% of the local effect. Moreover, the half-maximal stimulation of I_{Ca} was attained at 30-100 nM ISO applied locally, but required 0.3-1 μM ISO when applied distantly. This shows that both the efficacy and the potency of ISO to stimulate I_{Ca} are strongly increased by local application of the drug. Our data suggest that there is a non-uniform concentration of cAMP within a myocyte exposed to ISO, the concentration of cAMP being ≈10-fold higher near the Ca channels than in the rest of the cell.

M-AM-G3

β2-ADRENERGIC REGULATION OF THE CARDIAC Ca^{2+} CHANNEL STUDIED USING A STABLE CO-EXPRESSION SYSTEM. ((♥H. Masaki, *S. Green, + J. Heiny, *S. Liggett and ♥A. Yatani)) ♥Dep. of Pharmacol. & Cell Biophys., *Dep. of Medicine (Pulmonary), and +Dep. Mol. & Cellular Physiology, Univ. of Cincinnati, Cincinnati, OH 45267. (Sponsored by A. Bahinski)

In native cardiac myocytes, β1- and β2-adrenergic receptors (AR) coexist and participate in the regulation of contractile force and heart rate. The β1-AR activates cardiac Ca^{2+} channels (CaCh) via a cytoplasmic cAMP-dependent phosphorylation pathway and also through a direct G-protein/CaCh mechanism. The role of the β2-AR in modulating CaCh function is not known. To investigate β2-AR stimulation of the cardiac CaCh in a system with a single receptor subtype, we stably co-transfected Chinese hamster fibroblast (CHW) cells with cardiac CaCh α1 and β subunits and the β 2-AR. Untransfected cells showed no mRNA for CaCh subunits or AR's. Transfected cells expressed voltage-dependent DHP-sensitive currents characteristic of native CaCh's. Addition of a PKA inhibitor (H-89) did not reduce the currents, similar to the channel behavior in native cells, and consistent with the idea that the expressed channels are not maximally phosphorylated. Dialysis with the catalytic subunit of PKA produced a large increase in current amplitude. After partial activation of PKA by exogenous kinase; application of isoproterenol (Iso) increased the current with a biphasic time course. Under conditions where all phosphorylation pathways were blocked, forskolin or 8 Br-cAMP did not increase current amplitude; however, subsequent application of Iso rapidly increased current amplitude by over 50 %, suggesting a fast membrane-delimited G-protein mechanism. These results show that, like β1-AR, the β2-AR can modulate cardiac CaCh through multiple pathways.

M-AM-G4

ACTIVATION OF ADENOSINE A_1 RECEPTOR INHIBITS ONLY *N*-TYPE Ca^{2+} CURRENT IN RAT NEUROHYPOPHYSIAL TERMINALS. ((G.Wang and J.R.Lemos)) Worcester Foundation for Experimental Biology, 222 Maple Avenue, Shrewsbury, MA 01545.

We have shown that ATP, which is released from nerve terminals, could inhibit the neurohypophysial Ca^{2+} current. Since there is ecto-ATPase activity on these nerve terminals, we investigated whether this inhibition was by adenosine on a specific type of Ca^{2+} channel using the perforated patch-clamp technique. The two components (*N*- and *Q*-type) of the transient Ba^{2+} current were specifically blocked by 600 nM ω-CgTx GVIA, and 300 nM ω-Aga IVA or 100 nM ω-CgTx MVIIC, respectively. Application of 200-2000 μM adenosine partially inhibited the transient Ba^{2+} current with little or no effect on the long-lasting (*L*-type) Ba^{2+} current. Either 2000 μM adenosine or 100 μM of the A_1 receptor agonist 2-Chloroadenosine (2-CA) suppressed the isolated transient Ba^{2+} current by *ca.* 50%. The P_{2y} receptor agonist 2-Methylthio-ATP had no effect, however. ω-CgTx GVIA had no further effect on the adenosine- or 2-CA-resistant transient Ba^{2+} current, which could, however, be fully blocked by the addition of ω-Aga IVA. These results suggest that inhibition of synaptic neurotransmission by activation of A_1 receptors might be the result of a specific block of *N*-type, but not *L*- or *Q*-type, Ca^{2+} channels. (Supported by NIH grant NS29470)

M-AM-G5

THE α_1-SUBUNIT OF THE CARDIAC L-TYPE CALCIUM CHANNEL IS THE TARGET FOR MODIFICATION BY CYCLIC-AMP-DEPENDENT PROTEIN KINASE. ((W. Yuan, L. Cribbs, E. Perez-Reyes and D. M. Bers)) Loyola University Chicago, Maywood, IL 60153.

Cardiac L-type Ca current (I_{Ca}) is regulated by cAMP-dependent protein kinase (PKA), but the location of the regulatory site is not known. We tested the hypothesis that the cardiac α_1-subunit itself contains this site. We studied PKA modulation of I_{Ca} in tsA201 cells which were transiently transfected with the cardiac α_1-subunit (pRC-Caα_1). Untransfected cells do not express voltage-dependent I_{Ca} even with Bay K8644 and/or forskolin. In contrast, α_1-transfected cells expressed large dihydropyridine-sensitive currents (3-6pA/pF, 10mM Ba). Racemic Bay K 8644 (1 μM) caused ~4-fold enhancement of peak I_{Ba} and nifedipine (10 μM) blocked virtually all I_{Ba}. Forskolin stimulated I_{Ba} in only a few transfected cells, but the selective PKA inhibitors, H-89 (1 μM) or Rp-cAMPs (50 μM) normally led to a rapid decrease of I_{Ba} amplitude (Fig). Washout of H-89 did not result in spontaneous recovery of I_{Ba}, but the current was then readily activated by forskolin to near control values (Fig). Our data show that a) the tsA201 expression system is useful for studying the regulation of cloned L-type Ca channels and b) that the PKA regulatory phosphorylation site resides on the α_1 subunit of the channel.

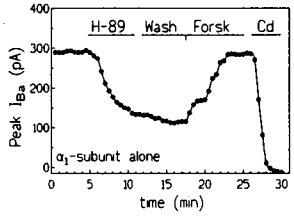

M-AM-G6

WITHDRAWAL OF ACETYLCHOLINE ELICITS A REBOUND INCREASE IN L-TYPE Ca^{2+} CURRENT ($I_{Ca,L}$) AND HYPERPOLARIZATION-ACTIVATED INWARD CURRENT (I_f) IN ATRIAL PACEMAKER CELLS. ((Y.G. Wang and S.L. Lipsius)) Loyola University Medical Center, Maywood, IL 60154

Termination of vagal nerve activity can elicit atrial tachycardia or premature atrial beats. We used a perforated patch whole-cell recording method to study the effects of acetylcholine (ACh) on $I_{Ca,L}$ and I_f recorded in SA node (SAN) and latent atrial pacemaker (LAP) cells. Pacemaker cells were isolated from cat right atria and studied at 35°C. Basal peak $I_{Ca,L}$ in SAN (8.2±1.0 pA/pF;N=8) and LAPs (6.7±0.5 pA/pF;N=16) and basal I_f amplitudes in SAN (5.3±0.3 pA/pF) and LAPs (4.2±0.6 pA/pF) were not different between the two types of pacemaker cells. In SAN, withdrawal from a 2 min. exposure to 1 μM ACh elicited a rapid rebound increase in $I_{Ca,L}$ (+32%) and I_f (+21%), above control (see Figure). Currents recovered to control levels within 4-5 min. LAPs also exhibited a rebound increase in $I_{Ca,L}$ (+50%) and I_f (+20%). In addition, action potentials showed that withdrawal of 1 μM ACh elicited a rebound increase in pacemaker rate in both SAN (+39%) and LAP (+66%). We conclude that rebound stimulation of $I_{Ca,L}$ and I_f in both SAN and LAPs may directly contribute to atrial tachycardia and premature atrial beats elicited upon termination of vagal nerve activity.

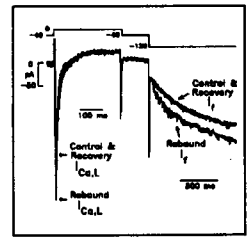

M-AM-G7

TRANSMITTER ACTIVATION OF AN INWARDLY-RECTIFYING K^+ CURRENT IN ACUTELY DISSOCIATED HIPPOCAMPAL NEURONS. ((D.L. Sodickson and B.P. Bean.)) Dept. of Neurobiology, Harvard Medical School, Boston MA 02115.

Serotonin, somatostatin, 2-chloro-adenosine, and the $GABA_B$ agonist baclofen activated an inwardly-rectifying K^+ current in freshly-dissociated hippocampal CA3 neurons. Baclofen-activated current rectified strongly with a voltage -dependence that shifted with $[K]_o$, reversed near E_K and was blocked by external Cs^+ and Ba^{2+} in a highly voltage-dependent manner. Current was activated by R(+)-baclofen (EC_{50} ~ 5 μM) with a lag followed by an exponential phase. τ_{on} decreased from ~2-3 secs at 500 nM baclofen to a limiting value of ~300 msec at 50 μM baclofen. Current deactivated with a time constant of ~0.5-1 sec, independent of agonist concentration. Somatostatin-induced current decayed much more slowly (τ~ 10 sec), probably reflecting higher affinity agonist binding.

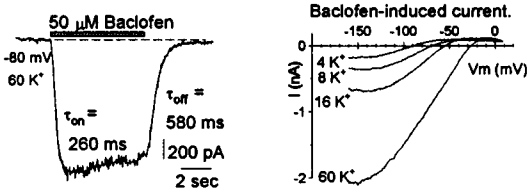

M-AM-G8

MODULATION OF SINGLE CHANNEL SUBSTATES OF CARDIAC INWARD-RECTIFIER K^+ CHANNELS BY Ca_i. ((M. Mazzanti, R. Assandri, A. Ferroni and D. DiFrancesco)) Dept. Physiology and Biochemistry, State University of Milano, I-20133 Milano, Italy.

The cardiac inward rectifier (IR) potassium channel passes little outward current during depolarizing voltage steps. It is known that rectification depends on the intracellular concentration of divalent ions such as Ca^{2+} and Mg^{2+}. However, the number of single-channel current substates present both in the inward and outward direction of current flow is still controversial. Some reports (Matsuda, 1987, Nature 325, 156) indicate a fully-open channel conductance of 21 pS and 3 outward current sublevels in the presence of intracellular Mg^{2+}. This has led to the proposal that IR channels have a 3-barrel structure (Matsuda et al., 1989, J. Physiol. 413, 139). On the other hand, we (Mazzanti and DiFrancesco, 1987, Pflügers Arch. 413, 322) and others (Sakmann and Trube, 1984, J. Physiol. 347, 641) previously recorded 4 substates and a fully-open conductance near to 28 pS. In the present study we used cell-attached and inside-out patch-clamp experiments on freshly dissociated guinea-pig ventricle myocytes to investigate the number of channel current sublevels, both in the inward and outward direction. Cells were superfused with a high K^+ (140 mM) solution to nullify resting potential and patch electrodes filled with the same solution. We found that in cell-attached single-channel inward current recordings showing substates, the 1st, 2nd and 3rd substate appear frequently, whereas the 4th (fully-conductive) substate appears only rarely. All sublevels contribute a constant conductance of about 7 pS. Patch excision in divalent-free solution increases the open probability of the 4th current level and abolishes all other sublevels in the inward as well as in the outward direction. Submicromolar concentrations of Ca^{2+} ions added to the internal side of the membrane induce reappearance of 4 single-channel current sublevels.

Supported by MURST and CNR.

M-AM-G9

$G_{q/11}$ MEDIATES SUBSTANCE P-INDUCED INHIBITION OF THE INWARDLY RECTIFYING K^+ CURRENT IN NUCLEUS BASALIS NEURONS. ((K. Takano, J. Yasufuku-Takano, T. Kozasa, W.D. Singer, P.C. Sternweis, S. Nakajima, and Y. Nakajima)) Dept. of Anat. and Cell Biol., Dept. of Pharmacol., Univ. of Illinois at Chicago, Chicago, IL 60312 and Dept. of Pharmacol., Univ. of Texas Southwestern Medical Center, Dallas, TX 75235.

Substance P (SP) induces a slow excitation of cultured nucleus basalis neurons by inhibiting an inwardly rectifying K^+ current (K_{IR}), mediated through a pertussis toxin (PTX)-insensitive G protein (Nakajima *et al.*, PNAS, 85:3643, 1988). To determine which specific type of PTX-insensitive G protein mediates this response, we conducted intracellular antibody injection with an Eppendorf microinjector and performed experiments with whole-cell voltage clamp. Antibodies were raised against peptide sequences at the carboxyl terminus of $G_{i2}\alpha$ or $G_{i3}\alpha$, and the common carboxyl terminal sequence of $G_q\alpha$ and $G_{11}\alpha$. In control neurons injected with preimmune IgG, SP application inhibited the membrane conductance due to the suppression of K_{IR} (32 ± 13 % inhibition, mean ± S.D., n=19). In contrast, the SP effect on K_{IR} was drastically reduced (3 ± 5 % inhibition, n=19) in neurons injected with anti-$G_{q/11}\alpha$ antibody. The SP effect on the neurons injected with the anti-$G_{q/11}\alpha$ antibody that was neutralized with its antigen peptide was similar (40 ± 17 % inhibition, n=10) to the SP effect on control neurons, indicating that the binding of the antibody to an endogenous G protein α subunit was responsible for the reduction of the SP response. SP effects on neurons injected with anti-$G_{i2}\alpha$ antibody (35 ± 13 % inhibition, n=13) and those injected with anti-$G_{i3}\alpha$ antibody (38 ± 13 % inhibition, n=9) were not significantly different from the control. Thus, the SP-induced inhibition of K_{IR} is mediated through $G_q\alpha$ or $G_{11}\alpha$.
Supported by NIH grant AG06093.

M-AM-G10

ISOPROTERENOL ACCENTUATES ACETYLCHOLINE-ACTIVATED INCREASES IN K^+ CONDUCTANCE VIA A GLIBENCLAMIDE-SENSITIVE K^+ CURRENT IN CAT ATRIAL MYOCYTES. ((Y.G. Wang and S.L. Lipsius)) Loyola University Medical Center, Maywood, IL 60154 (Spon. by K. Byron)

Cholinergic inhibition of the heart is accentuated by prior ß-adrenergic receptor stimulation via inhibition of cyclic AMP, i.e. accentuated antagonism. A perforated patch whole-cell recording method was used to study the effects of isoproterenol (ISO) on acetylcholine (ACh)-activated increases in K^+ conductance (gK^+). We compared gK^+ activated by an initial 30 sec. ACh exposure (ACh-1) with gK^+ activated by a second 30 sec. ACh exposure (ACh-2) separated by a 6 min. recovery interval. Voltage clamp ramps (40 mV/s) between -130 and +30 mV were used to assess total membrane conductance. In control, 10 μM ACh-1 and ACh-2 elicited increases in gK^+ that were not different from one another. When L-type Ca^{2+} current ($I_{Ca,L}$) was activated during the recovery interval, ACh-1 and ACh-2 still elicited similar increases in gK^+. However, with 1 μM ISO plus $I_{Ca,L}$ ACh-2 induced significantly larger increases in gK^+ than ACh-1. Forskolin (1 μM) exerted effects similar to those of ISO. The ACh-2-activated gK^+ potentiated by ISO was selectively abolished by: 1) 1 μM propranolol, 2) 50 μM Rp-cAMPs, 3) 1 μM ryanodine, 4) zero external Ca^{2+}, or 5) 10 μM glibenclamide. We conclude that ISO accentuates ACh-induced increases in gK^+ by enhancing Ca^{2+} influx and stimulating SR Ca^{2+} uptake via production of cyclic AMP. Elevated SR Ca^{2+} stimulates ACh to activate a glibenclamide-sensitive K^+ current, presumably due to ATP-sensitive K^+ channels. This mechanism may contribute to accentuated cholinergic inhibition induced by prior ß-adrenergic stimulation in atrial muscle.

M-AM-H1

BIOCHEMICAL CHARACTERIZATION OF α_1-β INTERACTION SITES IN VOLTAGE-DEPENDENT Ca^{2+} CHANNELS. ((M. De Waard, D.R. Witcher, M. Pragnell, H.Y. Liu and K.P. Campbell)) Howard Hughes Medical Institute, Dept. of Physiology and Biophysics, University of Iowa College of Medicine, Iowa City, IA 52242.

The α_1 and β subunits are integral components of two purified voltage-sensitive Ca^{2+} channels, the skeletal muscle dihydropyridine receptor and the neuronal ω-conotoxin GVIA receptor. Voltage-sensitive Ca^{2+} channel subunits have been separated into distinct classes based on molecular differences in α_1 (classes S, A, B, C, D and E) and β (β_1, β_2, β_3 and β_4) subunits. Despite the extreme functional and molecular diversity of Ca^{2+} channel subunits, it was recently demonstrated that β subunits bind to the cytoplasmic linker between repeats I and II of four distantly related α_1 subunits on an 18 amino-acid conserved motif (Pragnell *et al.*, Nature 368, 67-70, 1994). Also, the corresponding domain on β subunits that interacts with this α_1 motif was identified and localized to the amino-terminus of the second region of high conservation of all β subunits (De Waard *et al.*, Neuron 13, 495-503, 1994). We have now biochemically characterized the interaction between these two subunits. Glutathione-S-Transferase fusion proteins containing the α_1 motif were covalently coupled to Sepharose beads and used in a binding assay with *in vitro* translated β subunits. All β subunits specifically bound to the α_1 motif with a sub-nanomolar affinity. This interaction occurs with a half-time of association of 54 minutes at 4°C. It can be inhibited by a synthetic peptide of the α_1 motif. Once the β subunit had bound to the α_1 motif, the interaction was irreversible. It could however be partially reversed by the application of an excess α_1 motif peptide. A fusion protein containing the α_1 motif is also capable of inhibiting the native interaction in oocytes expressing a combination of α_{1A} and β_{1b} subunits.

M-AM-H2

IDENTIFICATION AND PURIFICATION OF β SUBUNITS OF VOLTAGE-DEPENDENT CA^{2+} CHANNELS USING THE α_1 SUBUNIT INTERACTION DOMAIN. ((D.R. Witcher, M. De Waard, H.Y. Liu, and K.P. Campbell)) Howard Hughes Medical Institute, Dept. of Physiology and Biophysics, University of Iowa College of Medicine, Iowa City, Iowa 52242.

β subunits of voltage-dependent Ca^{2+} channels play an important role in regulating Ca^{2+} channel function. The sites of α_1-β subunit interaction have been recently localized to cytoplasmic domains of both subunits (Pragnell *et al.*, Nature 368, 67-70, 1994 and De Waard *et al.*, Neuron 13, 495-503, 1994). The α_1 subunit interaction domain (AID) is an 18 amino acid conserved motif located between repeats I and II on all the α_1 subunits. In order to study the interaction of the β subunit with the AID, we have expressed a 50 amino acid Glutathione-S-Transferase (GST) fusion protein from the region of the I-II loop that contains this domain. A mutant fusion protein that contains a single amino acid change (Y392S) in the AID was also produced. These two fusion proteins along with GST were coupled to glutathione Sepharose beads to form affinity beads that were used in an *in vitro* binding assay to identify β subunits. The AID affinity beads but not the control or Y392S beads specifically bind β subunits from detergent extracts of different tissues (skeletal muscle, cardiac muscle, and brain). Affinity-purified rabbit and sheep antibodies directed against specific regions of β_1, β_2, β_3, and β_4 were used to analyze which β subunits bind to the AID epitope in each tissue homogenate. Affinity bead assays also demonstrate that AID beads bind to β subunits from tissue homogenates extracted with low salt and no detergent. Furthermore, this AID motif covalently coupled to CNBr Sepharose is useful in purifying β subunits from skeletal muscle. Thus, our data suggest that β subunits are not always associated with α_1 subunits of voltage-dependent Ca^{2+} channels.

M-AM-H3

AUXILIARY SUBUNITS FUNCTION AS A MOLECULAR SWITCH FOR GATING BEHAVIOR OF UNITARY N-TYPE CURRENTS. (M. Wakamori and Y. Mori) IMPB, Univ. of Cinti., Cinti., OH45267

Diverse gating behaviors underly the functional plasiticity of N-type Ca channels. We examined effects of auxiliary subunits α_2 and β on the unitary N-type activity directed by the BIII α_1 subunit (α_{1B}) in *Xenopus* oocytes. When the membrane potential was stepped from -100 mV to +20 mV, using 110 mV Ba^{2+} as the charge carrier, the gating patterns of unitary currents observed for the N-type channels were affected by different subunit combinations. The pattern of unitary currents produced by α_1+β was long opening (τ_o = 2.3 ms) with high opening probability (Po), whereas with α_1+α_2 a short opening pattern (τ_o = 0.5 ms) with low Po was observed. The combination of α_1+α_2+β or α_1 alone produced unitary currents with gating properties ranging between those of α_1+α_2 and α_1+β in terms of Po and τ_o. These results suggest that auxiliary subunits, in part, constitute a "molecular switch" for multiple gating modes.

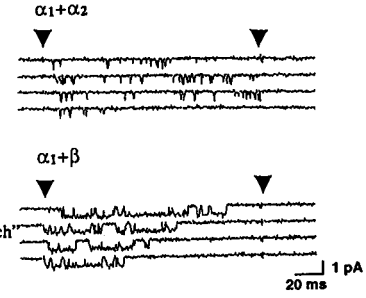

M-AM-H4

AN ESSENTIAL STRUCTURAL DOMAIN FOR Ca-SENSITIVE INACTIVATION OF L-TYPE Ca CHANNELS ((M. de Leon, L. Jones, E. Perez-Reyes, X. Wei, T.W. Soong, T.P. Snutch, and D.T. Yue)) Johns Hopkins University School of Medicine, Baltimore, MD 21205

Ca-sensitive inactivation is a crucial physiological feature of L-type Ca channels whereby Ca^{2+} influx accelerates inactivation. Our recent single-channel studies hint that Ca^{2+} binding to a cytoplasmic region of the channel initiates the inactivation process (Imredy and Yue, *Neuron*, 1994), but firm molecular evidence for such a site has so far been lacking. Presumed cytoplasmic regions of the α_{1C} subunit of the rabbit cardiac L-type Ca channel contain a single EF-hand Ca^{2+} binding motif (Babitch, *Nature*, 1990), which is only partially conserved in a rat brain Ca channel (α_{1E} , Soong et al, *Science*, 1993) notable for a lack of Ca-sensitive inactivation. Here we demonstrate selective ablation of Ca-sensitive inactivation in a chimeric Ca channel α_1 subunit ($\alpha_{1C.E.1}$), produced by substitution of the α_{1E} C-terminus (containing an analog of the EF hand) into a parent α_{1C} construct. Panel **A** illustrates the functional knockout: HEK 293 cells transfected with $\alpha_{1C.E.1}$+β_2 subunits yield normalized Ca^{2+} vs. Ba^{2+} currents that superimpose. In contrast, with α_{1C}+β_2, there is a prominent boost in the inactivation of Ca^{2+} vs. Ba^{2+} currents (**B**), indicative of robust Ca inactivation. Single-channel properties of $\alpha_{1C.E.1}$+β_2 differ strikingly from those of α_{1C}+β_2 when Ca^{2+} serves as charge carrier (but not Ba^{2+}): modal shifts synonymous with Ca inactivation are entirely absent. Reassuringly, other properties of the chimeric $\alpha_{1C.E.1}$+β_2 channel, like gating charge movement and voltage-dependent inactivation, are closely similar to those of α_{1C}+β_2, arguing against global derangement of conformation in the chimeric channel. These results give new reason to expect that Ca^{2+} binding to the α_{1C} subunit initiates Ca inactivation.

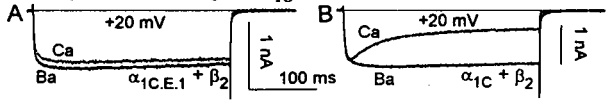

M-AM-H5

SINGLE AMINO ACID SUBSTITUTIONS IN A CHIMERIC DHP RECEPTOR ALTER ITS VOLTAGE SENSITIVITY. ((J. García⁺, J. Nakai⁺·*, K. Imoto* & K.G. Beam⁺)) ⁺Colorado State University, USA and *Kyoto University, Japan.

The S4 segments of the dihydropyridine receptor (DHPR) contain positively charged amino acids and are prime candidates for voltage sensing by the DHPR. We have characterized the effects of substituting a single glutamine (Q) for arginine (R) in repeats I (R168Q, R171Q) and IV (R1362Q, R1365Q) on Ca^{2+} currents and charge movement (Q) produced by the chimeric DHPR SkC15. In SkC15, the first repeat and the internal loops have skeletal origin, while the rest is cardiac-derived. Dysgenic myotubes, transiently expressing mutated DHPRs, were studied with the patch clamp technique. All the mutants decreased the amplitude of the expressed Ca^{2+} current. Repeat I mutants slowed calcium current activation (measured at 20-30 mV). R171Q shifted activation by +13 mV. Except for decreasing the amplitude, repeat IV mutants did not affect Ca^{2+} current activation. Repeat IV mutants had little effect on Q (repeat I has not been tested yet). We also studied Ca^{2+} currents and transients for a different group of repeat I mutants: substitution of glutamate (E) for arginine 171 (R171E), and substitutions of single valines (V) for leucines (L) in the leucine-heptad region (S4-S5 linker; L182V and L196V). R171E and L182V caused a depolarizing shift in the current activation curve and decreased its steepness. L182V slowed the kinetics of activation of the current while R171E had the opposite effect. R171E also shifted the curve of the Ca^{2+} transient to positive potentials with less effect on the steepness. L196V caused a negative shift in activation of current and transient activation curves with no significant change in the steepness. These preliminary results suggest that each repeat may have a different role in the functions of the DHPR. Supported by NIH (24444 & 28323).

M-AM-H6

SIGNIFICANCE OF DOMAIN IV FOR L-TYPE CALCIUM CHANNEL ACTIVATION REVEALED BY CHIMERIC CHANNELS FROM RABBIT CARDIAC AND CARP SKELETAL MUSCLE (CSKM) α_1-SUBUNITS. ((Z. Wang, A. Savchenko., M. Grabner, M. Froschmayr, S. Hering and H. Glossmann)) Institut für Biochemische Pharmakologie, Peter Mayr Straße 1, A-6020 Innsbruck, Austria

Chimeric calcium channel α_1-subunits consisting of: i) domain I and II from rabbit heart (*H*) and domain III and IV from Cskm (*C*) (*HHCC*); ii) domain I, II, III from heart and domain IV from Cskm (*HHHC*) and iii) domain I, II, IV from heart and domain III from Cskm (*HHCH*) were expressed after cRNA injection in *Xenopus laevis* oocytes. The activation kinetics, steady-state activation and inactivation parameters of chimeric calcium channel currents were estimated with two micro electrode voltage clamp technique in 40 mM Ba^{++}-solution. Inward currents recorded after expression of the chimeras *HHCC* and *HHHC* activated slowly with a time course which is typical for skeletal muscle calcium channels. Activation kinetics of inward currents during depolarising voltage steps from -80mV to 10mV (see figure) was described by two time constants (τ_1=27±2.5 ms, τ_2=294.±40.48 ms, n=7) compared to the fast and monoexponential activation of Ba^{++}-currents after expression of chimera *HHCH* or the pure cardiac α_1-subunit (τ_{HHCH}= 6,7±0.45 ms and τ_{HHHH}=6,31±0.28 ms, n=4). These results demonstrate that domain IV of the α_1-subunit is an important structural component determining the activation gating properties of L-type calcium channels.

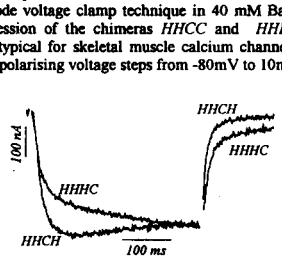

Supported by FWF grants S6601-MED (H.G.) and S6603-MED (S.H.), A.S. is a Lise Meitner Fellow.

M-AM-H7

LOCALIZATION OF THE SEQUENCE IMPORTANT IN SKELETAL-TYPE EC COUPLING IN THE II-III LOOP OF THE DHP RECEPTOR.

((J. Nakai+*, T. Tanabe, K.G. Beam+)) +Dept. of Physiol., Colorado St. Univ., *Dept. of Med. Chem., Kyoto Univ., Japan and Howard Hughes Med. Inst. and Dept. of Cellular and Molec. Physiol., Yale Univ. Sch. of Med.

Previous work has identified that the region between repeats II and III of the skeletal DHP receptor (DHPR) is an important determinant of skeletal-type EC coupling. To localize the critical region further, we made II-III loop chimeras between skeletal and cardiac DHPRs. Dysgenic myotubes expressing the chimeric DHPR were subjected to simultaneous measurement of calcium current and calcium transient using the whole cell patch-clamp technique with Fluo-3 in the patch pipette. When Ca^{2+} currents were blocked with Cd^{2+} and La^{3+}, CSk54 and CSk56 showed depolarization-induced calcium transients indicative of skeletal-type EC coupling; in contrast, CSk39 and CSk40 showed cardiac-type EC coupling. The overlapping region between CSk54 and CSk56 is only 17 amino acids long and is very important for skeletal-type EC coupling. Supported by Ministry of Education, Science and Culture, Inst. of Physical and Chem. Res., Japan; and the US NIH (NS24444).

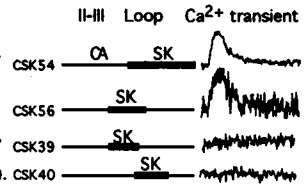

M-AM-H8

THE FUNCTIONAL REGULATION SITE OF SR Ca^{2+} RELEASE CHANNEL ON THE DHPR α1 SUBUNIT.

((J.P. Wang, A.Seryshev, Y.Wu, *N. Malouf, and S.L. Hamilton)) Dept. of Molecular Physiology & Biophysics, Baylor College of Medicine, Houston, TX and *Dept. of Biology, Univ. of N.C. at Chapel Hill, NC.

In the mechanical model of skeletal muscle E-C coupling, the cytoplasmic regions of dihydropyridine receptor (DHPR) directly or indirectly interact with the Ca^{2+} release channel. To elucidate these interactions we have prepared a series of synthetic peptides and expressed proteins corresponding to putative cytoplasmic sequences of the DHPR α1 subunit. A multi-antigenic peptide which corresponds to the residues 1487-1506 of DHPR α1 subunit inhibits the binding of [^{3}H]ryanodine to SR membranes. The IC_{50} for this effect is 45 ± 18 μM (n=3). The peptide also slows the dissociation of [^{3}H]ryanodine from high affinity binding sites. Using molecular cloning techniques, the polypeptides which correspond to residues 1382-1628, residues 1627-1873, and the II-III cytoplasmic loop of DHPR α1 subunit were expressed in *E.coli*. The purified II-III loop peptide enhances the [3H]ryanodine binding as previously reported by *Lu et al.* (1994), but the polypeptide 1382-1628 inhibits [^{3}H]ryanodine binding, suggesting the possibility that both regions of the DHPR α1 subunit can directly interact with the Ca^{2+} release channel. We have previously isolated and characterized a 14S tryptic digest of the Ca^{2+} release channel composed only of the peptides from Ca^{2+} release channel after Arg4475. The DHPR α1 subunit peptide, 1487-1506, slows the dissociation of [^{3}H]ryanodine from the 14S complex, suggesting that the site interaction of this peptide with the Ca^{2+} release channel is at C-terminal region of the channel after Arg4475. (This work is supported by grants from M.D.A. and N.I.H. AR41802, AR41729 and HL37044)

M-AM-H9

GATING CURRENTS OF RECOMBINANT CARDIAC L-TYPE CALCIUM CHANNELS EXPRESSED IN HUMAN EMBRYONIC KIDNEY (HEK-293) CELLS: RELATIONSHIP BETWEEN CHARGE MOVEMENT AND IONIC CURRENT.

((R. Bangalore*, G. Mehrke#, K. Gingrich*, F. Hofmann#, and R.S. Kass*)) Dept. of Physiology*, U. of Rochester, Rochester, NY, 14642; and Inst. Pharm. und Toxikolgie#, Tech. U.Munchen, 80802 Munchen, Germany.(Spon. by I. Sarelius)

We have studied the relationship between ionic current and charge movement in HEK 293 cells transiently transfected with cDNA's encoding the α_1C, α_2, and β2a subunits of the L-type calcium channel. HEK 293 cells were co-transfected (lipofection) with individual cDNA's. L-type channel currents could be recorded 2 to 3 days post transfection with whole cell patch clamp procedures. Ionic currents measured in the presence of 20 mM Ba^{2+}, were characterized by activation and inactivation kinetics similar to native channels. Non-linear charge movement, measured in (mM) nominally 0 Ca^{2+}, 5 Cd^{2+}, 5 Mg^{2+}, and 0.1 La^{3+}-containing solutions, was detected and identified as L-channel gating current by the following criteria: $Q_{on} = Q_{off}$; charge moved saturated (Q_{max}) at positive potentials, was not observed in L-channel-free cells; and could be inactivated by depolarization. Charge movement preceded activation of ionic currents: Boltzmann fits to ionic current (G) and charge movement (Q) activation yielded $V_{1/2}$ (mV) values of 4.4±2 (5)(G) and -10.83±2(3)(Q); and effective valences of 3.95±0.3 (7) (G) and 2.33±0.4(3)(Q). These values are consistent with properties of α_1 β-injected Xenopus oocytes(Neely, et al., Science 262: 575-577, 1993). However, we find Gmax/Qmax = 45.3 ±11(3), a value within the range reported for α_1 encoded channels in oocytes. Our results suggest that mammalian cell processing of L-channels may differ from that of Xenopus oocytes, and that the role of the β subunit in regulating channel function may differ in the two expression systems.

M-AM-H10

INSIGHTS INTO CALCIUM CHANNEL ACTIVATION FROM SPECTRAL ANALYSIS.

((R. T. Dirksen and K. Beam)) Dept. Physiol., Colo. St. Univ., Fort Collins, CO 80523.

Activation kinetics of macroscopic currents are ~20 times slower for skeletal L-type calcium channels than for cardiac. This slow activation could occur as a result of fast closed-closed transitions followed by a slow transition into (and out of) the open state. Such a scheme (right) would predict a τ_{ACT} of $1/(\alpha+\beta)$ as well as long open times for channels manifesting slowly activating macroscopic current. We previously compared in dysgenic myotubes the unitary behavior of expressed skeletal and cardiac channels in which P_o was increased by BayK 8644. The skeletal and cardiac channels both exhibited short and long open times (at 0 mV: 2.2 and 28.5 ms for skeletal and 3.9 and 12.5 ms for cardiac). If the longer openings contributed significantly to the total current, then a model like that above could account for slow activation. To determine whether long openings were also significant in the absence of BayK, we performed stationary fluctuation analysis (final 400 ms of 500 ms test pulses) on multi-channel, cell-attached patches containing either rapidly activating cardiac channels or slowly activating chimeric channels (SkC15: Repeat I skeletal, Repeats II-IV cardiac). Power spectra were fit by the sum of two Lorentzians with corner frequencies (Fc), at +10 mV, of 45.2 ± 8.3 and 658.9 ± 47.1 Hz for SkC15 and 91.4 ± 8.9 and 790.4 ± 66.5 Hz for cardiac. From these Fc's, mean open times of 3.5 and 0.2 ms, and 1.7 and 0.2 ms were calculated for SkC15 and cardiac channels, respectively. The lack of long open times, in the absence of BayK, means the model depicted above cannot account for slow activation. The addition of BayK caused an increase in low frequency power for both SkC15 and cardiac channels. The resulting spectra were well fit by the sum of three Lorentzians, yielding calculated open times at (+10 mV) of 19.4, 1.4, and 0.2 ms for SkC15 and 18.5, 1.6, and 0.2 ms for cardiac. Thus, BayK stabilizes an additional, long-lived open state for both channel types, but this long open state is not critical for slow activation of skeletal L-current. Supported by grants AR08243 to RTD and NS24444 to KB.

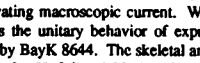

MEMBRANE FUSION: EXOCYTOSIS AND ENDOCYTOSIS I

M-AM-I1

EXOCYTOSIS AND CALCIUM HOMEOSTASIS AT A SLOW SYNAPSE.

((F. Rieke and E. A. Schwartz)) Dept. of Pharmacology and Physiology, The University of Chicago, Chicago, IL 60637.

Rod photoreceptors release transmitter during darkness and decrease release during illumination. Absorption of a single photon in a salamander rod produces a 30-100 μV hyperpolarization lasting approximately 1 sec, a signal that is 1000 times smaller and longer lasting than the presynaptic signal in a spiking cell. Thus synapses in spiking cells and rod photoreceptors have different functional tasks. We have studied exocytosis in rod terminals by a combination of Ca^{2+} imaging, capacitance measurement, and photolysis of caged Ca^{2+}. Photolysis of nitr-5 raised the Ca^{2+} concentration to 1-2 μM and increased the capacitance 50-200 fF. Thus moderate Ca^{2+} concentrations are sufficient to trigger exocytosis in rods. We measured steady-state Ca^{2+} concentrations in the synaptic terminal at voltages near the dark resting potential of -40 mV. The spatially averaged Ca^{2+} concentration at -40 mV was 2-4 μM and decreased e-fold for a 4 mV hyperpolarization. Thus the cytoplasmic Ca^{2+} concentration maintained during physiological conditions reaches levels sufficient to produce exocytosis. As a result, exocytosis is controlled by Ca^{2+} influx through voltage-gated channels, Ca^{2+} extrusion across the plasmalemma, and intracellular Ca^{2+} stores.

M-AM-I2

CALCIUM-ION DYNAMICS AT PRESYNAPTIC ACTIVE ZONES OF HAIR CELLS.

((Naoum P. Issa and A. J. Hudspeth)) Howard Hughes Medical Institute and Southwestern Medical School, Dallas, TX 75235-9117.

Exocytosis of neurotransmitter molecules is triggered by the influx of Ca^{2+} at presynaptic active zones. The entry of Ca^{2+} at individual active zones can be studied with exceptional temporal and spatial resolution in the mechanosensory cell of the auditory system, the hair cell. The Ca^{2+} indicator fluo-3 specifically labels the hair cell's active zones, and thus provides a highly sensitive measure of local Ca^{2+} entry there. By simultaneously monitoring the whole-cell Ca^{2+} current and fluo-3 fluorescence intensity during depolarizing pulses, we measured the time course of Ca^{2+} entry and diffusion. With large depolarizations, the Ca^{2+} concentration approximately 200 nm from the presynaptic membrane approached steady state with a time constant of less than 10 ms. Because the space constant of fluo-3 fluorescence was less than the sectioning depth of the confocal imaging system, we developed a numerical algorithm to compensate for the effects of out-of-focus fluorescence. Application of this algorithm to fluorescence profiles obtained by rapidly scanning across a maximally stimulated active zone indicated that the local Ca^{2+} concentration reached about 100 μM. Inclusion in the whole-cell pipette of an exogenous Ca^{2+} buffer, such as BAPTA or EGTA, slowed the approach to steady-state fluorescence and restricted the spread of fluorescence from the presynaptic membrane. Both the concentration and the *on* rate of an exogenous Ca^{2+} buffer affected the steady-state fluorescence and Ca^{2+} concentration. Further experiments should permit the quantification under physiological conditions of the Ca^{2+} concentration in the immediate vicinity of individual presynaptic active zones.

This work was supported by NIH grant DC00317.

M-AM-I3

EXOCYTOSIS AND ENDOCYTOSIS OF SINGLE 60 NANOMETER VESICLES RESOLVED AS STEPWISE CAPACITANCE CHANGES. ((K. Lollike[1], N. Borregaard[1] and M. Lindau[2])) [1]Dept. of Internal Medicine and Haematology L, Rigshospitalet, DK-2100 Copenhagen, Denmark & [2]MPI f. med. Forschung, D-69120 Heidelberg, Germany.

In whole cell recordings capacitance steps >2 fF associated with exocytosis of single granules >300 nm can be resolved. However, most secretory vesicles and granules have a diameter of 60-300 nm, corresponding to capacitance steps of only 0.1-2.3 fF We measured capacitance changes in cell attached patches of human neutrophils using a high frequency lock-in method. With this technique the noise level is reduced to 0.025 fF such that capacitance steps of 0.1 fF are clearly detected corresponding to exo- and endocytosis of single 60 nm vesicles. It is thus possible to detect almost all known exocytotic and endocytotic processes including exocytosis of small neurotransmitter containing vesicles in most cell types, as well as endocytosis of coated and uncoated pits. In neutrophils we demonstrate a stepwise capacitance decrease generated by 60-165 nm vesicles as expected for endocytosis of coated and non-coated pits. Following ionomycin stimulation a stepwise capacitance increase is observed consisting of 0.1-5 fF steps corresponding to the different granule types of human neutrophils from secretory vesicles to azurophil granules. The opening of individual fusion pores is resolved during exocytosis of 200 nm vesicles. The initial conductance has a mean value of 150 pS and can be as low as 35 pS, similar to the conductance of ion channels.

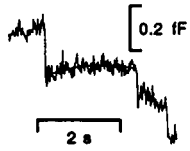

M-AM-I4

RAPID CAPACITANCE CHANGES IN NERVE TERMINALS. ((Shyue-fang Hsu and Meyer B. Jackson)) Department of Physiology, University of Wisconsin, Madison WI 53706.

We measured capacitance changes in nerve terminals from posterior pituitary thin slices using phase tracking techniques. Capacitance changes induced by 200 ms pulses from -90 to 10 mV at one minute intervals declined in two phases. In the first phase, lasting two minutes, stimulus-induced capacitance changes declined to 50% of the first response recorded after break-in. Subsequently, evoked capacitance changes declined slowly, and were still 45% of the initial value 14 minutes after break-in. We examined the relationship between Ca^{2+} influx and capacitance change, with voltage varied between -50 to 50 mV. The voltage of maximum capacitance change was well correlated with the peak in the Ca^{2+} current-voltage plot. Increasing pulse duration between 12.5 and 350 ms increased capacitance changes, with significant saturation. However, the saturation was entirely accounted for by inactivation of Ca^{2+} current. Plotting capacitance change versus charge influx (obtained from the integral of Ca^{2+} current) gave an excellent linear dependence, indicating no depletion of exocytosis-ready vesicles in this time period. Fast endocytosis was initiated immediately following termination of stimulus. Capacitance decayed exponentially with a time constant between 0.2 and 1 s. In some terminals, after longer pulses endocytosis was slower. This may reflect inhibition of fast endocytosis by Ca^{2+} (von Gersdorff and Matthews, Nature, 370, 652, 1994).

M-AM-I5

RAPID ENDOCYTOSIS IS Ca^{2+}- AND GTP-DEPENDENT IN ADRENAL CHROMAFFIN CELLS AND IS BLOCKED BY ANTI-DYNAMIN BUT NOT BY ANTI-CLATHRIN ANTIBODIES. ((C. R. Artalejo[1], J. Henley[2], M. McNiven[2], H. C. Palfrey[3])) [1]Dept. Neurobiol. & Physiol., Northwestern U., Evanston, IL; [2]Cent. Basic. Res. Digest. Dis., Mayo Clinic, Rochester, MN; [3]Dept. Pharmacol. & Physiol. Scis., U. Chicago, Chicago, IL. (Spon. by P. Loach)

Exocytosis-endocytosis coupling was monitored in cultured bovine adrenal chromaffin cells by patch recording of cell capacitance. Depolarizing trains that activated Ca^{2+} channels result in secretion manifest as stepwise increases in capacitance (C. R. Artalejo et al, Nature 365, 72, 1994). On termination of the stimulus capacitance decreased rapidly in a process defined by two time constants of ~0.3 and ~3 or ~3 and ~13 sec. in different cells. Typically the original pre-stimulation cell capacitance value was regained, suggesting that rapid endocytosis (RE) precisely matches exocytosis of membrane under these conditions. When Ba^{2+} or Sr^{2+} rather than Ca^{2+} were used as charge carriers, secretion was not significantly affected but RE was abolished, suggesting that RE is Ca^{2+}-dependent and that the Ca^{2+} receptors for exocytosis and endocytosis must be different. The regulation of RE was investigated by introducing various reagents into the cell *via* the patch pipette. Removal of GTP or inclusion of GTPγS or GDPβS to block guanine nucleotide turnover on G-proteins eliminated RE without significantly affecting exocytosis. As dynamin is a G-protein that has been implicated in other forms of endocytosis we introduced affinity-purified, epitope-specific anti-dynamin antibodies into the cell. These also resulted in a complete blockade of RE. Fab fragments of anti-dynamin IgG were also inhibitory but preimmune IgG was without effect. Immunochemical analysis showed that chromaffin cells express abundant dynamin. By contrast, introduction of monoclonal anti-clathrin antibodies into the cell had no effect on RE. RE was also unaffected by low internal pH (pHi 6.2), which blocks receptor-mediated endocytosis. The latter results suggest that clathrin-coated vesicles are not involved in RE.

M-AM-I6

IMAGING OF RAPID MEMBRANE RETRIEVAL FOLLOWING EXOCYTOSIS IN SEA URCHIN EGGS. ((Tim Whalley and Steven. S. Vogel)) LTPB, NICHD, NIH, Bethesda, MD 20892.

Cells which undergo massive exocytosis maintain cell surface area via subsequent endocytosis. Little is known about how these cellular processes are linked. One way to link these two processes and maintain membrane surface area during secretion would be to close fusion pores after exocytosis. We have investigated this hypothesis in sea urchin eggs which upon fertilization discharge the contents of approximately eighteen thousand 1.3 μm diameter cortical secretory granules in response to the release of Ca^{2+} from intracellular stores. Using confocal microscopy in conjunction with a fluorescent fluid phase marker rhodamine dextran and fluorescent lipid phase markers FM 1-43 and RH 414, we have observed the direct and rapid retrieval of plasma membrane into 1.5 μm vesicles. This retrieval can be triggered by fertilization with sperm, or by egg activation with the calcium ionophore A23187. The half time for this membrane retrieval mechanism is approximately 5 minutes and we have never observed it in the absence of cortical granule exocytosis. The magnitude of this retrieval process is about 6% of the eggs starting volume and thus can account for the changes in plasma membrane surface area caused by exocytosis. The mechanism of this membrane retrieval process is not via clathrin-coated pits, it is not stimulated by treatment with the protein kinase C activator PMA (known to trigger the formation of coated pits in sea urchin eggs) but the reaction is inhibited by procaine, an inhibitor of cortical granule exocytosis. These results together with labelling experiments using sequential pulses of fluid phase markers suggest that homeostatic membrane retrieval is achieved via fusion and the eventual resealing of exocytotic fusion pores, and suggests that the phenomenon of fusion pore 'flicker' may be physiologically important for maintaining cell volume and surface area.

M-AM-I7

ENDOCYTOSIS IS CALCIUM-DEPENDENT IN A SYNAPTIC TERMINAL. ((H. v. Gersdorff & G. Matthews)) Dept. Neurobio., SUNY, Stony Brook, NY 11794.

Exocytosis and endocytosis were studied by measuring the associated increase and recovery in the membrane capacitance of acutely isolated synaptic terminals of goldfish retinal bipolar neurons. To drive secretion, Ca-current was activated with depolarizing voltage-clamp pulses from a holding potential of −60 mV to 0 mV (1 sec duration and given at arrows in Fig.), and the size of the resulting capacitance increase was measured. With $[Ca^{2+}]_i$ = 100 nM capacitance recovers rapidly to baseline after a stimulus (exponential time constant τ = 2 sec; see Nature 370, 652-655). However, as shown in the Fig., when $[Ca^{2+}]_i$ was buffered through the patch pipette to = 1 μM (a range acheivable by Ca-current activation), capacitance did not recover. Endocytosis is thus strongly inhibited by elevated $[Ca^{2+}]_i$. The rate of membrane retrieval was found to be steeply dependent on $[Ca^{2+}]_i$, with a Hill coefficient of 4 and half-inhibition at ~500 nM. At $[Ca^{+2}]_i$ › 900 nM, endocytosis is completely absent. This action of internal calcium on endocytosis represents a negative-feedback mechanism controlling the rate of membrane recovery in synaptic terminals after neurotransmitter secretion. (Supported by NIH grant EY03821 and NRSA Fellowship EY6506).

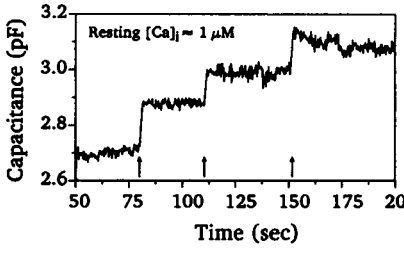

M-AM-I8

DYNAMIN IN *DROSOPHILA MELANOGASTER*: TWO ISOFORMS ASSOCIATED WITH DIFFERENT INTRACELLULAR COMPARTMENTS IN WILD-TYPE AND *SHIBIRE^{TS}* NEURAL TISSUE. ((G.V. Gass-Gritsenko[1], J. J.-C. Lin[1] R. Scaife[2], and C.-F Wu[1])) Dept. of Biological Sciences, Univ.of Iowa, Iowa City, IA 52242, USA, [2]Institut de Biologie Structurale, 38027 Grenoble, France.

The temperature-sensitive mutations of the *shibire* (*shi*) gene in *Drosophila* cause endocytic arrest, resulting in neurotransmission block and paralysis at high temperatures. We examined the subcellular distribution of dynamin, a product of the *shi* gene by immunoblotting and immunocytochemical assays using two antibodies directed against different regions of dynamin. Two isoforms of dynamin with apparent M_r of 92 kD and 94 kD have been detected in wild-type and temperature sensitive (*shi^{ts}*) adult neural tissue. The two isoforms were reproducibly associated with different subcellular pellet fractions of head homogenates and relatively little dynamin could be detected in the supernatant after high speed (130,00 X g) centrifugation. The 94 kD isoform represents the majority (60-70%) of total dynamin and appears to be membrane-associated. It can be extracted from the low speed (2,000 X g) membrane pellet by high salt, Na_2CO_3 (pH 11) or Triton X-100 treatments. Extracted 94 kD dynamin is able to re-associate with artificial phospholipid vesicles. The 92 kD isoform cannot be released by high salt or Na_2CO_3 treatments, suggesting a different mechanism of association with cell structures. The distribution of the two isoforms is not altered by the presence of stabilized microtubules in homogenates. No apparent degradation or subcellular redistribution of mutant dynamin was detected in two *shi^{ts}* alleles after heat shock or block of the dynamin GTPase activity, suggesting that intracellular redistribution or degradation of mutant dynamin are not involved in the endocytosis arrest in these mutants. The results suggest that the two isoforms do not appear to correspond to different functional states of dynamin but are likely to be involved in different cellular compartments within the membrane cycling pathway.

M-AM-I9

IONIC FLUXES IN ENDOCYTIC VESICLES OF RABBIT RETICULOCYTES. ((E.M. Besser, D.M. Rimmer, C.D. Boethel, J.S. Weeks, T.C. Moore, C-Y, Li, J.A. Watkins, and J. Glass)) Center for Excellence in Cancer Research, Treatment, and Education, Hematology/Oncology Section, LSUMC-S, Shreveport, LA, 71130.

The regulation and control of endosomal acidification is a rate limiting process of iron absorbtion via transferrin processing and has been implicated in vesicular targeting. Reticulocyte endosomes provide a relatively simple model for investigating detailed relationships among ionic fluxes, membrane potential generation ($\Delta\Psi$), and pH gradient formation (ΔpH). Based on current models of endosomal ionic fluxes, the kinetic effects of inhibitors, nucleotides, and buffer conditions have been examined with respect to Cl^- and Na^+ fluxes, rates and extents of ΔpH and $\Delta\Psi$ generation, and formation of mononucleotides. Kinetically significant perturbation but not abolition of $\Delta\Psi$ generation was observed with DIDS, DCCD, NEM, and strophanthidin which are inhibitors of the Cl^- channel, proton pore, H^+-ATPase hydrolysis, and Na^+/K^+-ATPase or Na^+ channel respectively. In contrast, acidification was substantially inhibited by these agents.. Nigericin, valinomycin, FCCP, and monensin, ionophores for Na^+/H^+ exchange, K^+, H^+, and K^+/Na^+ exchange, affected $\Delta\Psi$ generation by 89±9%, 353±35%, and 209±21% while DCCD, DIDS, NEM, and the ionophores nigericin and monensin significantly inhibited acidification. Under conditions where only 1 mM ATP or GTP was added, formation of up to 5 nmoles/mg protein of the mononucleotides was detected. In addition, cyclic AMP and GMP increased both the rates and extents of the observed kinetics by at least one order of magnitude. These results provide a basis for extending our current models for detailed stoichiometric investigation. Supported by NIH DK-37866.

BIOCHEMISTRY AND MECHANICS OF MUSCLE CONTRACTION I

M-AM-J1

3-ISOBUTYL-1-METHYLXANTHINE (IBMX) ENHANCES 5-HYDROXY-TRYPTAMINE (5-HT) EFFECTS ON ADULT RAT VENTRICULOCYTES. ((H.E. Reuben, P. Paolini, E. Béjar)) Department of Biology, San Diego State University, San Diego, CA 92115 and Rees-Stealy Research Foundation, San Diego, CA 92101.

5-HT exerts direct positive inotropic and chronotropic effects on the rat heart. The receptor(s) and signal transduction mechanism(s) responsible for these effects have not yet been elucidated. The cardiac 5-HT_4 receptor type causes an increase in cAMP associated with increased contractility. Overall cell shortening and sarcomere kinetics are obtained by computer-assisted video imaging analysis. Ventriculocytes are isolated by perfusing through the coronary circulation with a modified Krebs-Henseleit solution supplemented with collagenase. The cells are incubated in buffer supplemented with 1 mM Ca^{++} and 50 µM pargyline, a monoamine oxidase (MAO) inhibitor. The cells are then electrically paced, videotaped and analyzed. Cumulative concentration response curves (CCR) are constructed for 5-HT in the presence and absence of 5 µM IBMX and/or 10 µM atenolol. IBMX was found to increase the positive inotropic response of 5-HT at 1 µM with 12.34 ± 0.63 % shortening as opposed to a 4.49 ± 2.50 % in the absence of IBMX, suggesting that cAMP is involved in the signal transduction. Atenolol, a β_1-adrenergic antagonist, does not block 5-HT-mediated effects. (Supported by grants from the Rees-Stealy and California Metabolic Research Foundations.)

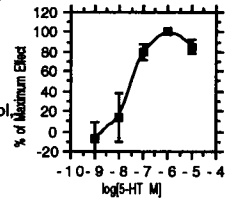

M-AM-J2

LOAD DEPENDENT ACTIVATION OF MITOGEN-ACTIVATED PROTEIN KINASE IN VASCULAR SMOOTH MUSCLE. ((L.P. Adam, M.T. Franklin and D.R. Hathaway)) Krannert Institute of Cardiology and the Dept. of Physiology, Indiana University, Indianapolis, IN 46202.

Stimulation of contractile smooth muscle by KCl and phorbol esters results in the activation of mitogen-activated protein kinase (MAPK). Several lines of evidence suggest that MAPK in the vasculature phosphorylates the thin filament binding protein, h-caldesmon. Phosphorylation of h-caldesmon occurs at two sites in the carboxyl terminus of the protein, and we have hypothesized that phosphorylation of h-caldesmon may be required for sustained tension. Basal MAPK activity is high in unstimulated carotid arteries that are incubated in a physiological saline solution and stretched on a force transducer (activity is approximately 100 pmole/min/mg protein when assayed using a peptide substrate specific for MAPK). On the other hand, MAPK activity in arteries that are freeze-clamped in vivo (i.e., without dissection), or dissected, rinsed and immediately freeze-clamped is low (approx. 11 pmole/min/mg). In order to explain this phenomenon, strips of artery were subjected to various initial loads and MAPK activity was determined. In muscles incubated at 37°C, MAPK activity was proportional to the initial load applied to the muscle reaching a maximum value at approximately 16 x 10^3 N/m^2. The time required for the increase in MAPK activity was rapid, reaching a peak within 30 seconds. The mechanisms through which load activates MAPK activity are unknown. However, these data show that MAPK activity in vascular smooth muscle is regulated in response to both pharmacological stimulation and mechanical load.

M-AM-J3

A SERIES-TO-PARALLEL TRANSITION DURING THE RISE OF ACTIVATION OF SMOOTH MUSCLE. (V.R. Pratusevich, C.Y. Seow, & L.E. Ford)) Univ. of Chicago, Chicago, IL 60637

If smooth muscle thick filaments are evanescent, dissolving partially during relaxation and reforming during activation, they must lengthen as they reform. This lengthening would place more crossbridges in parallel on each filament and require fewer filaments in series to span the length of the muscle. Such a series-to-parallel transition could cause the velocity slowing that occurs during tetanic force development. To test if this transition could account for the slowing, force-velocity relations were measured at different times during the rise of tetanic force. The reference data obtained at the beginning of the plateau of the tetanus were fitted to the Hill hyperbola using a non-linear, least-squares technique. These reference curves could be fitted exactly to test data obtained at the other times by using the same factor to scale force downward and velocity upward after correcting for differences in activation. The correction was made by multiplying the test isotonic forces by the ratio of maximum power in the reference data to that in the test data. It assumes that the crossbridge cycling rate does not change during the tetanus and that all activated bridges contribute to power, irrespective of whether they are in series or in parallel. The first assumption is contrary to the prevalent theories that crossbridge cycling rate slows during a tetanus, and the proposed transition is thus an alternative to these theories. The goodness of the fit indicates that the proposed transition can account for the data at least as well as the metabolic theories.

M-AM-J4

EFFECTS OF TEMPERATURE ON CROSS-BRIDGE KINETICS IN SMOOTH MUSCLE. ((A. Arner and Å. Österman)) Dept Physiology and Biophysics, Lund University, Sweden. (Spon. by B. J. Rydqvist)

Effects of temperature on mechanical properties of skinned muscle from the guinea-pig taenia coli were investigated in order to obtain information about temperature dependent steps in cross-bridge interaction in smooth muscle. In maximally thio-phosphorylated fibres, force was decreased by about 10% at 30 °C and by about 30% at 2 °C, relative to values at 22 °C. The maximal shortening velocity (Vmax) was increased by 90% at 30 °C and decreased by 50% at 5 °C (values relative to 22 °C). The rate of tension development from rigor was measured after rapid photolytic release of ATP from caged-ATP in thiophosphorylated fibres. Compared with 22 °C the rate of force development was decreased to 40 % at 5 °C and increased more than 3 times at 30 °C. We conclude that the reactions in the cross-bridge cycle determining the isometric force have comparatively little temperature dependence in smooth muscle. The effects of temperature on the rate of force generation after ATP release from caged-ATP suggest a high temperature dependence of a reaction occurring from the rigor state to force generation (including ATP binding, cross-bridge detachment and ATP-hydrolysis) in the smooth muscle fibre.

M-AM-J5

TEMPERATURE EFFECT ON ELEMENTARY STEPS OF THE CROSS-BRIDGE CYCLE IN RABBIT SOLEUS MUSCLE FIBERS. ((Gang Wang and Masataka Kawai)) Department of Anatomy, University of Iowa, Iowa City, IA 52242

Elementary steps of the cross-bridge cycle were investigated with sinusoidal analysis in skinned rabbit soleus slow-twitch fibers at varing temperatures (15-30°C). The muscle preparations were activated at pCa 4.4, ionic strength 180 mM, and the effects of MgATP (S), MgADP (D), and phosphate (P) concentrations on three exponential processes (*B,C,D*) were studied. Results are consistent with the following cross-bridge scheme:

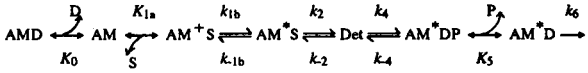

Where A=actin, M=myosin, D=MgADP, S=MgATP, P=phosphate. We found that K_0 (MgADP binding) and K_{1a} (MgATP binding) are 2.5X of rabbit psoas, and K_5 (Pi binding) is 0.5X of psoas, indicating that slow-twitch fibers are more resistant to ATP depletion and Pi accumulation. The rate constants of elementary steps are generally 6-25 times slower in soleus than in psoas. The equilibrium constant of force generation step K_4 increases significantly with a temperature increase, and this step accompanies a large enthalpy increase (155 kJ/mol), indicating that the force generation step consists of an endothermic reaction. This step also accompanies a large entropy increase corresponding to 530 J/mol/deg. These observations are consistent with the hypothesis that the hydrophobic interaction between residues of actin and myosin underlies the mechanism of force generation.

M-AM-J6

THE WHISTLE AND THE RATTLE: THE DESIGN OF SOUND PRODUCING MUSCLES ((L.C. Rome, D.A. Syme, S. Hollingworth, S. Lindstedt, S.M. Baylor)) Biology and Physiol., Univ. Penn. Phila. PA, 19104 & MBL, Woods Hole

Sound producing muscles must operate at 10-100-fold greater frequencies than do locomotory muscles in the same animal. For instance toadfish swim with 2-5 Hz tailbeat frequencies, while the swimbladder muscle (TSB) powers the "boat whistle" mating call at 100-200 Hz. Rattlesnakes move at 0.6 to 3 Hz while the shaker muscle (RS) rattles at 100 Hz. To understand the adaptations for faster twitches, we first examined the systematic changes in toadfish fibers (15-16°C) with twitch half-widths varying by 100-fold: 600ms for red muscle (TR); 90ms for white muscle (TW), and 6ms for swimbladder. The Ca^{2+} transient half-widths (measured with furaptra) varied by a similar ratio: ~200 ms for TR, 21 ms for TW, and 4.3 ms for TSB fibers. In addition, there was a systematic shift in force-pCa relationship of skinned fibers with increasing twitch speed. The pCa_{50} was 6.2 for TR, 5.7 for TW, and 5.3 for TSB. This right shift for the TSB likely reflects a faster off-rate of Ca^{2+} from troponin (k_{off}), which modelling suggests is necessary to permit relaxation. Finally, there was a progressive speeding up of crossbridge detachment rate as assessed by V_{max}: 2.2 ML/s for TR, 4-5 ML/s for TW, and 10-12 ML/s for TSB. These results suggest that the fast twitches require: (1) a brief troponin occupancy, which in turn requires a brief Ca^{2+} transient and fast k_{off}, and (2) a fast crossbridge detachment rate (i.e., high V_{max}.)

The shaker muscle seems to follow the same pattern of adaptation. At 15°C, the RS has a fast Ca^{2+} transient (4ms), but an unexceptional pCa_{50} (5.8) and V_{max} (6 ML/s), and hence can only produce 20 Hz twitches without summation. By contrast at 35°C, with a Ca^{2+} transient half-width of ~1.5 ms and V_{max}=~15 ML/s (pCa_{50} not measured at 35°C), they can produce 100 Hz twitches with little summation. In addition to rapid twitch kinetics, these adaptations permit the TSB and RS to generate positive work at the frequencies used--a necessity for sound production. NIH, NSF, and MRC.

M-AM-J7

CONTRACTILE PROTEIN FUNCTION IS DECREASED IN RATS WITH CHRONIC MYOCARDIAL INFARCTION. ((Pieter P. de Tombe, Thomas Wannenburg, William Litlle)) Bowman Gray School of Medicine, Winston-Salem, NC 27157.

Congestive heart failure (HF) is associated with decreased myocyte force generating capacity. The mechanism of the cellular dysfunction is presently unknown. Accordingly, we studied contractile function in cardiac trabeculae isolated from the right ventricles of rats with either experimental HF, induced by 24 wks chronic myocardial infarction (n=6), or from Sham operated rats (n=6). Sarcomere length (SL) was measured by laser diffraction techniques and force was measured by silicon strain gauge. SL was kept constant at all times by computer feedback control. HF was associated with marked left ventricular dilation and pulmonary congestion. In intact twitching trabeculae, HF was associated with a depression of the force-SL relation at $[Ca^{2+}]_0$=1.5 mM (top panel) and the force-$[Ca^{2+}]_0$ relation at SL=2.0μm (middle panel; $p<0.05$). HF was also associated with a significant depression of the force-$[Ca^{2+}]_i$ relation at SL=2.0 μm following chemical permeabilization of these trabeculae (bottom panel; $p<0.05$). We conclude that reduced myocyte force development in this model of heart failure is due, in part, to depressed function of the contractile filaments.

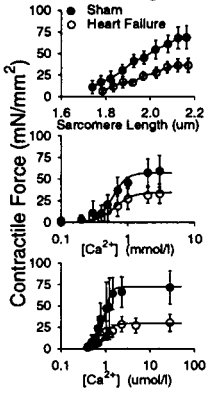

M-AM-J8

POLYETHYLENE GLYCOL PRODUCES LARGE INCREASES IN THE AMOUNT OF MYOSIN-S1 BOUND TO ACTIN DURING STEADY STATE ATP HYDROLYSIS. ((Howard White, Betty Belknap, Matthew Walker, and John Trinick)) Muscle Research Group, Bristol University School of Veterinary Medicine, Langford, Bristol, U.K. and Department of Biochemistry, Eastern Virginia Medical School, Norfolk, Va.

Polyethylene glycol (PEG) as been used to increase the affinity of dilute solutions of weakly interacting macromolecules. During steady state ATP hydrolysis the affinity of myosin for actin in dilute solution is extremely low at physiological ionic strength, resulting in complete dissociation of actomyosin by ATP. Studies of the mechanism of actomyosin ATP hydrolysis have in the past have partially circumvented this problem by using very low ionic strength, but there was always concern that the low ionic strength might affect other aspects of the mechanism than myosin binding to actin. PEG provides an alternative method of increasing the affinity of myosin for actin in the presence of substrate and may be of use in biochemical and structural studies of the interaction between actin and myosin at moderately high ionic strength. Addition of PEG to a solution of actomyosin-S1 increases the apparent affinity of S1 for actin during steady state ATP hydrolysis. This was indicated by a decrease in the Kapp of actin-activated ATP hydrolysis of up to 25 fold at optimal concentrations of PEG, while the maximum rate of hydrolysis was unchanged. Higher concentrations of PEG produced a decrease in the maximum rate of hydrolysis. An increase in S1 binding to actin during steady state ATP hydrolysis is also observed by electron cryo-microscopy. This work was supported by HL41776 and the American Heart Association.

M-AM-J9

PRESTEADY STATE ELECTRON MICROSCOPY OF mant-ATP BINDING TO ACTO-MYOSIN-S1 USING A RAPID SPRAY-MIX-FREEZE-QUENCH-METHOD. ((Matthew Walker, Howard White, and John Trinick)) Muscle Research Group, Bristol University School of Veterinary Medicine, Langford, Bristol, U.K. and Department of Biochemistry, Eastern Virginia Medical School, Norfolk, Va. 23507. (Spon. by Wei Jiang)

We recently obtained electron micrographs of actomyosin-S1 rapidly frozen during steady state ATP hydrolysis (Walker et al, Biophys J., 66, 1563-1572, 1994). The pictures showed considerable disorder, which suggests the myosin head may adopt more than one conformation while going through the ATPase cycle. We have now begun to obtain micrographs of the acto-S1 complex frozen in defined kinetic states. This allows exploration of whether the different kinetic states are associated with particular structural geometries. We have chosen to use the substrate analogue mant-ATP ((2'(3')-O-)N-methylanthraniloyl)-ATP because the maximum rate of dissociation of acto-S1 dissociation by this substrate, measured by stopped-flow light scattering is 150 s^{-1} at 4° C, which is ten fold less than ATP. During the 5-10 ms between spraying a grid containing acto-S1 with mantATP and freezing, nearly all of the acto-S1 will have bound mantATP but 25-50 percent of the myosin-S1 will not have dissociated from actin. Moreover, there will not have been time for a significant amount of hydrolysis to occur. Under such conditions we have been able to observe S1-mantATP is bound to actin with a variety of configurations, as was previously observed during steady state hydrolysis of ATP. This work was supported by a grant from the American Heart Association and a Fogarty Senior International Fellowship to HW.

M-AM-K1

Ca^{2+} MEASUREMENTS IN *LIMULUS* VENTRAL PHOTORECEPTORS USING LASER CONFOCAL MICROSCOPY.

((Kyrill Ukhanov and Richard Payne)) Dept. of Zoology, University of Maryland, College Park, MD 20742

Limulus ventral photoreceptors were pressure injected with 1 mM fluo-3, indo-1 or a mixture of 250 μM CaGreen5N with 10 mM ANTS, dissolved in 100 mM KAsp, 10 mM HEPES, pH 7.0. All measurements were performed on a Zeiss LSM 410 laser confocal scanning microscope using the 488 nm line of an Ar-Kr laser or 364 nm line of an Ar laser. The electrical response of the photoreceptors and a light monitor were also stored on a computer. The photoreceptor and the dye were simultaneously stimulated by a stationary laser spot, focused onto the most sensitive region of the photoreceptor. The volume within which the Ca signal was measured did not exceed 10 μm^3 (10^{-14}l). Under these conditions, the Ca signal rose simultaneously with the electrical response. The rate of rise of the Ca-signal exceeded that measured with conventional methods by 4-5 fold. The Ca signal peaked within 30-40 ms, rising nearly as fast as membrane depolarization. Positioning of the laser spot further from the most sensitive area of the R-lobe resulted in both a delay of the Ca signal and a decrease in its rate of rise. Using a line scanning mode, we observed that elevation of calcium spreads throughout the R-lobe, beginning at its outer rim, but that it barely enters the A-lobe, implying effective management by intracellular Ca-buffers within the A-lobe. By removal of extracellular calcium, we confirmed that the Ca signal arises from light induced Ca-release. We also verified our previous results on uncoupling of Ca-release and electrical excitation. When Ca-release was completely blocked by cyclopiazonic acid, a Ca-pump blocker, or by Ca-ionophore 4-Br-A23187, photoreceptors were still capable of producing electrical responses.

We conclude that spatial averaging does distort the timecourse of Ca-signals and that, although Ca release does not appear to be essential for excitation, it may rise under these conditions fast enough to participate in initiating the electrical response.

M-AM-K2

INVOLVEMENT OF CYCLIC GMP IN TRANSDUCTION IN HYPERPOLARIZING INVERTEBRATE PHOTORECEPTORS.

((Maria del Pilar Gomez and Enrico Nasi)) Department of Physiology Boston University School of Medicine and Marine Biological Laboratory Woods Hole MA (Spon by B. Kaminer)

The eye of *Pecten* possesses both depolarizing and hyperpolarizing photoreceptors. The latter share some similarities with vertebrate rods, both structurally (the transducing structure derives from modified cilia) and functionally (the photocurrent rectifies outwardly due to voltage-dependent block by divalent cations, and is inhibited by amiloride). We used patch electrodes to dialyze putative messengers of the transduction cascade into voltage-clamped, isolated ciliary photoreceptors. In sharp contrast with known rhabdomeric photoreceptors, calcium ions do not seem to play a crucial role in phototransduction: intracellular perfusion with 1-100 μM free Ca did not appreciably change the membrane current in the dark nor light responsiveness. BAPTA (10 mM) failed to suppress the photocurrent and to slow down its kinetics. The light response also survived prolonged (>1 hour) superfusion in Ca-free extracellular media, with repetitive photostimulation. Manipulations of the phosphoinositoid cascade were also ineffective: no currents were induced by internal application of IP_3 (1-10 μM), and the light response was seemingly unaffected by the antagonists heparin (1 mg/ml) and decavanadate (20 μM). By contrast, dialysis of 8Br cGMP (50-250 μM) induced an outward current, up to 1 nA, with an increase in membrane conductance. The stimulatory effects of 8Br cGMP were accompanied by a dose-dependent desensitization of the light response. Similar results could also be obtained with cGMP, but at higher concentrations (millimolar). The effects were not produced by 250 μM 8Br cAMP, suggesting nucleotide specificity. Activation of single channel currents by 8Br cGMP was observed in excised patches previously screened for the presence of light-activated channels. Supported by NIH grant RO1-EY07559.

M-AM-K3

LIGHT ADAPTATION IN *PECTEN* HYPERPOLARIZING PHOTORECEPTORS: INSENSITIVITY TO CA MANIPULATIONS.

((Enrico Nasi and Maria del Pilar Gomez)) Department of Physiology Boston University School of Medicine and Marine Biological Laboratory Woods Hole MA

The hyperpolarizing photoreceptors in the double retinas of some invertebrates display significantly lower light sensitivity and faster photoresponse kinetics than their depolarizing counterparts. In addition, these cells fail to produce quantum bumps in response to dim illumination. These features prompted the suggestion that they may already be in a light-adapted state at low light levels. We here demonstrate that the photocurrent of hyperpolarizing cells from *Pecten* displays all manifestations of sensory adaptation: (1) The response amplitude to a test flash is decreased in a graded way by background or conditioning lights. The attenuation, which is induced at intensities considerably above threshold, develops over tens of milliseconds. (2) Adapting stimuli shift the stimulus-response curve to the right and reduce the size of the saturating photocurrent. (3) The fall kinetics of the photoresponse are accelerated by light adaptation, and the roll-off of the modulation transfer function, measured with sinusoidal stimuli, is displaced to higher frequencies. Based on the notion that Ca mediates light adaptation in other cells, we examined the consequences of manipulating this ion. Removal of external Ca reversibly increased the photocurrent, without affecting basal sensitivity, kinetics, or light adaptation; the effect seems therefore to concern ion permeation, rather than the regulation of the visual response. Intracellular dialysis with 10 mM BAPTA did not reduce the peak-to-plateau decay of the photocurrent, or the background-induced response reduction. Conversely, high levels of buffered $[Ca]_i$ (1-10 μM) also spared the manifestations of light adaptation. Finally, preliminary observations using chelerythrine, a protein kinase C (PKC) specific inhibitor, do not support the notion that PKC is critical for light-adaptation. Supported by NIH grant RO1 EY-07559.

M-AM-K4

AMINO-TERMINAL MYRISTOYLATION INDUCES COOPERATIVE CALCIUM BINDING TO RECOVERIN.

((J.B. Ames, T. Porumb, T. Tanaka, M. Ikura, and L. Stryer)) Dept. of Neurobiology, Stanford Univ., Stanford, CA 94305 and Ontario Cancer Institute, Univ. of Toronto, Toronto, Ontario, Canada M4X 1K9.

Recoverin, a new member of the EF-hand superfamily, serves as a Ca^{2+} sensor in vision. A myristoyl or related N-acyl group covalently attached to the N-terminus of recoverin enables it to bind to disc membranes when the Ca^{2+} level is elevated. Ca^{2+}-bound recoverin prolongs the lifetime of photoexcited rhodopsin, most likely by blocking its phosphorylation. We report here Ca^{2+}-binding studies of myristoylated and unmyristoylated recombinant recoverin to help understand how the Ca^{2+}-myristoyl switch operates. Unmyristoylated recoverin exhibits heterogeneous and uncooperative binding of two Ca^{2+} with dissociation constants of 0.11 and 6.9 μM. In contrast, two Ca^{2+} bind cooperatively to myristoylated recoverin with a Hill coefficient of 1.75 and apparent dissociation constant of 17 μM. Thus, the attached myristoyl group lowers the calcium affinity of the protein and induces cooperativity in Ca^{2+} binding. One-dimensional ^1H NMR and two-dimensional ^{15}N-^1H shift correlation spectra of myristoylated recoverin measured as a function of Ca^{2+} concentration show that a concerted conformational change occurs when two Ca^{2+} are bound. The binding and NMR data can be fit to a concerted allosteric model in which the two Ca^{2+} binding sites have different affinities in both the T and R state. The T state buries the myristoyl group inside the protein. The R state places the myristoyl group outside so that it can interact with membranes. Ca^{2+} binds to the R state at least 10,000-fold more tightly than to T. The dissociation constants of the two sites in the R state of the myristoylated protein are 0.11 and 6.9 μM, as in unmyristoylated recoverin. The ratio of the unliganded form of T to that of R is estimated to be 400 for myristoylated and <0.05 for unmyristoylated recoverin. Thus, the myristoyl group serves as a covalently attached allosteric effector.

M-AM-K5

TOWARDS THE STRUCTURE OF THE MEMBRANE PROTEIN, RHODOPSIN.

((Philip L. Yeagle, James L. Alderfer, and Arlene D. Albert)) Department of Biochemistry, University at Buffalo, Buffalo, NY 14214; Department of Biophysics, Roswell Park Cancer Institute, Buffalo, NY 14263.

The structure of rhodopsin is essential to an understanding of visual transduction. Furthermore, rhodopsin is a member of the family of G-protein receptors. Considerable progress is being made on the structure of the transmembrane portion of rhodopsin. However, the region that is responsible for interaction of the receptor with the G protein in signal transduction is extramembraneous. We have approached the question of the structure of the extramembraneous portions of rhodopsin by determining the structure of those regions as if they were protein domains. The data accumulated to date support that hypothesis. Initially the carboxyl terminal segment (the last 33 amino acids on the carboxyl terminus of rhodopsin) was studied. The circular dichroism spectrum indicates that this carboxyl-terminal peptide has some β-like structure. This peptide inhibited the cGMP cascade, indicating that the peptide had structure with functional relevance. Therefore, high field multidimensional NMR studies were undertaken to determine the 3-dimensional structure of this peptide. The resulting structure is globular. Serines and threonines that can be phosphorylated are clustered. The structure opens a new discussion on the interaction between G proteins and their receptors and may offer a new paradigm for the determination of the structures of membrane proteins. (NEI EY03328)

M-AM-K6

SOLUBILIZATION AND RECONSTITUTION OF A GTPASE ACTIVATING PROTEIN FOR THE RETINAL G PROTEIN TRANSDUCIN

((Joseph K. Angleson and Theodore G. Wensel)) Verna & Marrs McLean Department of Biochemistry, Baylor College of Medicine, Houston, TX 77030 (Spon. by J. A. Malinski)

The α subunit of the visual G protein transducin ($G_{t\alpha}$) hydrolyzes bound GTP very slowly on its own, but hydrolysis can be accelerated by interactions with other proteins. We have found that rod outer segments contain a membrane protein that can greatly accelerate GTP hydrolysis by $G_{t\alpha}$ [Angleson, J. K., and Wensel, T. G. (1993) *Neuron,* **11**:939-949]. The activity of this GTPase accelerating protein (GAP) can be further enhanced by the γ subunit of the enzyme regulated by $G_{t\alpha}$, cGMP phosphodiesterase (PDE) [Angleson, J. K., and Wensel, T. G. (1994) *J. Biol. Chem.* **269**:16290-16296]. PDE_γ binds tightly to $G_{t\alpha}$ but has no effect on GTPase in the absence of the GAP. The solubility properties of the GAP are characteristic of an intrinsic membrane protein. Recently we have found conditions for reconstituting the GTPase accelerating activity of the GAP after detergent solubilization of rod outer segment membranes While the GAP can be separated from phospholipids in active form, it loses activity rapidly in detergent solution unless phospholipids are present. Supported by NIH Grants EY07981 & EY07001, and by the Welch Foundation.

M-AM-K7

SALAMANDER UV-SENSITIVE CONES UTILIZE MORE THAN ONE VISUAL PIGMENT ((C. L. Makino, R. L. Dodd, P. Rohlich, D. A. Baylor)) Dept. Neurobiology, Stanford Univ., Stanford, CA, 94305, Lab. of Electron Microscopy, Semmelweiss Univ. of Medicine, Budapest, Hungary.

In general, each vertebrate photoreceptor contains only a single type of visual pigment. The blue-sensitive cone of primate contains less than one copy in 10^5 of the red- and green-sensitive pigment molecules. The ultraviolet-sensitive cone in salamander, however, appears to be an exception. Action spectra of isolated, salamander rods and cones were determined with suction electrode recording or whole cell voltage clamp over the range 367 to 830 nm. The spectra of 9 UV-sensitive cones had a maximum below 370 nm, a shoulder near 450 nm and a secondary maximum near 600 nm. A shoulder and a secondary maximum were not present in the spectra of 17 rods, 57 red-sensitive cones or 15 blue-sensitive cones. Exposure of the UV-sensitive cone to light of wavelengths greater than 600 nm reduced the secondary maximum without changing the sensitivity to wavelengths shorter than 500 nm. Thus the UV-sensitive cone contains at least 2 functional visual pigments. Assuming similar photosensitivities, the red-sensitive component comprises less than one in 10^3 of the total visual pigment content. (Supported by NEI)

M-AM-K8

THE P_{Ca}/P_{Na} PERMEABILITY RATIO IS HIGHER IN CGMP-GATED CHANNELS OF CONE PHOTORECEPTORS THAN IN THOSE OF RODS. ((A. Picones and J. I. Korenbrot)) Dept. of Physiology, University of California, San Francisco, CA 94143

We have proposed that differences in the phototransduction signals of rods and cones reflect quantitative differences in the homeostasis of cytoplasmic Ca^{++} between the two photoreceptor types (Curr. Opin. Neurobiol. 4:488 (94)). In particular, we have hypothesized that, under identical driving force, the fraction of the current carried by Ca^{++} through the cGMP-gated channels of the cone outer segment is about twice that in the channels of rod outer segment (J. Gen. Physiol. 104: (94)). We tested this thesis by measuring ion selectivity ratios in membrane patches detached from outer segments of either single cones from striped bass or rods from tiger salamander. Under symmetric solutions of NaCl (160 mM), we measured the reversal potential of currents elicited by 1 mM cGMP in the presence of varying concentrations of $CaCl_2$ between 0 and 15 mM. Elevated Ca^{++} both blocked the current amplitude and shifted the reversal potential. The blocking effect of Ca^{++} is quantitatively similar in cones and rods. At +50 mV, blocking is well described by a Michaelis-Menten function with a $K_{1/2}$ of about 1.1 mM in cones and 1 mM in rods (Tanaka and Furman, J. Memb. Biol. 131:245 (93)). The shift in reversal potential, on the other hand, is much larger in cones than in rods. Using the constant field equation, the computed P_{Ca}/P_{Na} selectivity ratio is essentially independent of Ca^{++} concentration, and its value is about 8.5 in cones but it is only about 2.5 in rods.

M-AM-K9

CROSS-LINKING OF Na-Ca-K EXCHANGER AND cGMP-GATED CHANNEL OF BOVINE ROD OUTER SEGMENTS.

((Paul J. Bauer)) Institut für biologische Informationsverarbeitung, Forschungszentrum Jülich, P.O.B. 1913, D-52425 Jülich, Germany.

Both Na-Ca-K exchanger (NaCaK-Ex) and cGMP-gated channel (cG-channel) of rod outer segments (ROS) are located in the plasma membrane. The cG-channel is a heterooligomer consisting of several α-subunits and at least one β-subunit, the latter being part of a protein with the apparent molecular weight (m.w.) of 240kD (240kD protein). It has been suggested that NaCaK-Ex and cG-channel are associated (Bauer & Drechsler, J. Physiol. 451, 109, 1992). I have carried out chemical cross-linking on washed ROS membranes to examine this notion. The α-subunit, the 240kD protein, and the NaCaK-Ex were probed with the following monoclonal antibodies (gifts of Drs. L. and R. Molday): PMc 2G11, PMs 5SE11, PMex 2D9, respectively. Several reagents bridging primary amino residues yielded adducts of α-subunits of the cG-channel but did not cross-link α-subunits and the 240kD protein or α-subunits and the NaCaK-Ex. Cross-linking of thiol groups yielded adducts with the 240kD protein and adducts with the NaCaK-Ex but not with α-subunits. Upon thiol cross-linking, three extra bands were observed for the NaCaK-Ex with the apparent m.w. of 320kD, 380kD, and 480kD, the highest having twice the m.w. of NaCaK-Ex. Neurominidase treatment shifted these bands by about 50 kD to lower m.w.. Copper phenanthroline catalysed oxidation of thiol groups yielded the same additional bands for the NaCaK-Ex. These results indicate that disulfide bonds are likely to be involved in the quaternary structure of NaCaK-Ex and cG-channel in ROS plasma membranes. Their functional role is currently investigated.

VIRUS STRUCTURE AND ASSEMBLY

M-AM-L1

STRUCTURAL BASIS OF CAPSID MATURATION OF BACTERIOPHAGE HK97. ((J.F. Conway[1], R.L. Duda[2], N. Cheng[1], R.W. Hendrix[2], and A.C. Steven[1])) [1]Lab. of Structural Biology Research, NIAMS, Bethesda, MD 20892; and [2]Dept. of Biological Sciences, University of Pittsburgh, Pittsburgh, PA 15260, USA. (Spon. by H. Pant)

The first complete precursor of the HK97 capsid, Prohead I, contains 415-420 copies of the major capsid protein (42kDa) arrayed in a T=7 icosahedral lattice with diameter ~470Å. Maturation starts with proteolytic cleavage of the capsid protein (42→32kDa) to produce Prohead II, which subsequently undergoes an "expansion" transformation to yield Head I (diameter of ~550Å). Autocatalytic covalent crosslinking between capsid proteins converts Head I into the final Head II. We have examined all four states of the maturing capsid by cryo-electron microscopy and three-dimensional reconstruction to resolutions of 25-30Å. Both Proheads are round, thick-walled, particles that are morphologically similar although Prohead II is ~2% larger. Their pentons observe 5-fold symmetry, but their hexons show a striking departure from 6-fold symmetry, as if a hexameric variant of the penton had been sheared into two trimers by a 20-25Å dislocation along a central plane. The amino-terminal domain excised in the Prohead I→II transition has been localized by difference mapping to the inner surface of the shell, where it consists in part of inwardly-directed extensions that emerge from each subunit and coalesce into a single aggregate per capsomer. The Prohead II→Head I transition is accompanied by major structural changes, including a ~15% increase in diameter; the initially round facets become almost planar; the hexons become 6-fold symmetric; and the shapes of the capsomers are radically transformed. These observations suggest the occurrence of major conformational changes in addition to changes in contacts with neighbors. In contrast, no structural differences between Head I and Head II are discernible at our present resolution.

M-AM-L2

ENTROPIC INTERACTIONS AND VIRAL CAPSID STABILITY: POINT MUTATIONS IN THE P22 BACTERIOPHAGE COAT PROTEIN WHICH DESTABILIZE SUBUNIT/SUBUNIT INTERACTIONS. ((Debora Foguel[1], Carolyn M. Teschke[2], Peter E. Prevelige Jr.[3], Jerson L. Silva[1])) [1]Departamento de Bioquimica, Universidade Federal do Rio de Janeiro; Rio de Janeiro, RJ 21941 - Brazil; [2]Dept of Molecular and Cell Biology, Univ. of Conn. 75 N. Eagleville Rd. Storrs, CT. [3]Boston Biomedical Research Institute, 20 Staniford St., Boston MA. 02114;

The Salmonella typhimuriuam bacteriophage P22 is a double-stranded DNA containing phage whose assembly pathway serves as a model for other dsDNA viruses such as herpes. The P22 morphogenetic pathway requires the formation of a precursor procapsid empty of DNA that subsequently matures into the capsid upon DNA packaging and a structural rearrangement. The stability of bacteriophage P22 coat protein in both monomeric and procapsid like forms to hydrostatic pressure has been previously examined (Prevelige, King, & Silva, Biophys. J., 1994, 66, 1631-1641). While the monomeric protein is unstable toward pressure the procapsid shell is very stable to applied pressur demonstrating the role of intersubunit contacts in subunit stability We have analyzed the pressure stability of procapsid shells composed of two single-amino acid substitution mutants in the coat protein (G232D and W48Q). The data demonstrate the importance of both hydrophobic interactions and cavities on virus capsid stability, and suggest the importance of these interactions in controlling virus assembly and uncoating

M-AM-L3

AN ALTERNATE TOROID-BASED MODEL FOR THE ORGANIZATION OF DOUBLE-STRANDED DNA IN BACTERIOPHAGE HEADS.

((Nicholas V. Hud)) Biology and Biotechnology Research Program, Lawrence Livermore National Laboratory, Livermore, California 94551, U.S.A.

Investigations of double-stranded DNA organization within bacteriophage heads have produced a wealth of biophysical and biochemical data. However, despite the development of numerous models with very distinct characteristics, not one model has been found to be simultaneously consistent with all presently available data. The observation of toroidal DNA structures in the electron micrographs of gently lysed phage heads has long been sited as support for the organization of DNA in a spool-like fashion. Such models are also attractive in terms of virus self-assembly, for toroids are readily produced *in vitro* when DNA is complexed with viral DNA-condensing agents. Toroidal packaging models for phage DNA, however, have received significant criticism because the results of several studies were found to be inconsistent with the spool model, not with the presence of toroids *per se*. Recently we developed a constant radius of curvature model for DNA organization within toroidal condensates produced *in vitro*, a model which represents a significant departure from the spool model. Applying our toroid model to the problem of how DNA is organized within bacteriophage heads has resulted in a model which is consistent with a wide range of biophysical and biochemical data. This work was conducted under the auspices of the U.S. Department of Energy Contract W-7450-ENG-48.

M-AM-L4

HSV CAPSID PROTEIN VP26 IS ABSENT FROM PENTONS : DIFFERENCE MAPPING BETWEEN VP26$^+$ AND VP26$^-$ CAPSIDS ASSEMBLED IN A RECOMBINANT BACULOVIRUS SYSTEM.

((B.L. Trus[1,2], F.L. Homa[3], D.R. Thomsen[3], W.W. Newcomb[4], F.P. Booy[1], J.C. Brown[4] & A.C. Steven[1])) [1] LSBR-NIAMS and [2] CBEL-DCRT, NIH, Bethesda, MD 20892; [3] Upjohn Co., Kalamazoo, MI 49001; [4] U. Va. Med. School, Charlottesville, VA 22908. (Spon. by Jay Miller).

The capsid of Herpes Simplex Virus Type 1 contains 960 copies of its major protein, VP5 (149 kDa), arrayed on a T=16 icosahedral surface lattice. 150 hexamers occupy the hexon sites and 12 pentamers, the penton sites [1]. Significant conformational differences exist between the penton and hexon states of VP5, as expressed in antigenicity, susceptibility to proteolysis, and ease of extraction with urea. Six copies of VP26 (12 kDa) bind around the outer tip of each hexon, as determined by difference mapping between 3-D reconstructions from cryo-electron micrographs [2]. However, because these experiments were performed with penton-less capsids, they did not reveal whether VP26 is also present on pentons. We have now performed similar experiments with capsids that do contain pentons and differ only in the presence/absence of VP26. The capsids were isolated from insect cells infected with recombinant baculoviruses carrying appropriate combinations of HSV1 genes. The resulting difference map shows positive density around the hexon tips, confirming our earlier result [2], but no density at the corresponding penton sites, indicating that VP26 is absent [3]. Thus the conformational differences between the penton and hexon states of VP5 extend to the VP26 binding site.

1. Newcomb, W.W., Trus, B.L., Booy, F.P. et al (1993) J. Mol. Biol. **232**, 499-511.
2. Booy et al, F.P., Trus, B.L., Newcomb, W.W. et al (1994) PNAS-USA **91**, 5652-6.
3. Zhou, Z.H., Prasad, B.V.V., Jakana, J. et al (1994) J. Mol. Biol. - in press.

M-AM-L5

REFINEMENT OF A MODEL FOR Pf1 VIRUS*.

((David J. Liu[1], Shun-Le Chen[2], and L.A. Day[1])) [1]The Public Health Research Institute, New York, NY 10016; [2]Dept of Molecular Biophysics & Biochemistry, Yale University, 260 Whitney Ave, New Haven, CT 06511.

A structural model of filamentous virus Pf1 that has helical coat protein and DNA with phosphates close to the structural axis (1), has been refined by means of the simulated annealing method (2) as implemented for processing fiber diffraction data (3). The starting model has the phasing of the two DNA strands that provides electrostatic stability (4), and leads to cancellation of diffraction on certain layer lines (1,4). The refinement combines restraints from published data from X-ray fiber diffraction and neutron diffraction, and from chemical labeling and various spectroscopies. Methods of restraining radial positions were developed. The refined model fits all experimental data within their limits of resolution. Refined against 3 Å X-ray fiber diffraction data (5), our model has R-factors below 0.3 and bond lengths and angles that are comparable to those found in well refined structures. The 3 Å data (5) produce a map with electron density assignable to DNA phosphates at 2.5 Å radius and to protein subunits that are exclusively helical.

(1) D.J. Liu and L.A. Day, *Science* **265**, 671 (1994), and references therein.
(2) A.T. Brünger, *X-PLOR Version 3.1* (1993).
(3) H. Wang and G. Stubbs, *Acta Cryst.* **A49**, 504 (1993).
(4) C.J. Marzec and L.A. Day, *Biophys. J.* **67(#6)**, in press (1994).
(5) D.A. Marvin, R.K. Bryan, and C. Nave, *J. Mol. Biol.* **193**, 315 (1987).
*Financial support from NIH grant GM42286.

M-AM-L6

PACKING OF COAT PROTEIN HELICES IN FILAMENTOUS BACTERIOPHAGE M13 AND IKE: ROLE OF SMALL RESIDUES IN PROTEIN OLIGOMERIZATION.

((K.A. Williams and C.M. Deber)) Research Institute, Hospital for Sick Children, Toronto M5G 1X8; and Department of Biochemistry, University of Toronto, Toronto M5S 1A8, Ontario, Canada.

Filamentous bacteriophage M13 and IKe are encapsulated by *ca.* 2700 copies of the 50 residue (53 in IKe) major coat protein (gene 8), which participates in helix-helix packing (a) while stably inserted into the *E. coli* inner membrane; and (b) between subunits upon assembly onto phage DNA in the lipid-free virion. To examine the molecular basis for these diverse interactions, we used a combination of randomized and saturation mutagenesis of the entire gene 8 of M13 and the hydrophobic segment of gene 8 in IKe, to assess the susceptibility of each position to mutation. In the resulting library of *ca.* 150 viable mutants, "small" residues (*ie.*, Ala, Gly and Ser) which line the non-polar surface of the N-terminal amphipathic helical segment of M13, together with those on the hydrophobic segments of both proteins were found to be highly conserved. These results support a model in which major coat protein participates in two principal types of protein-protein interactions in the phage; layer (tangential) contacts between the Ala-rich face of the N-terminal segment of one subunit and the corresponding face of the TM domain of a subunit two levels above, and axial (radial or lateral) contacts between adjacent monomers 16 Å out of register. Both interactions rely on a combination of bulky hydrophobic and small residues for stable helix-helix interactions. These studies are being complemented with direct biophysical characterization of wild type and mutant phage by circular dichroism and intrinsic tryptophan fluorescence.

M-AM-L7

MOLECULAR AND DOMAINAL ORGANIZATION OF A HINGED VIRAL ADHESIN

((M.E. Cerritelli, M.N. Simon*, J. F. Conway, and A.C. Steven)) LSB-NIAMS, NIH, Bethesda, MD 20892; *Brookhaven Nat'l Lab, Upton, NY 11973.

The long tail-fibers (LTFs) of bacteriophage T4 attach the virion to the host cell surface during infection. The LTF is a complex oligomeric fibrous protein that is rich in β–structure and assumes multiple conformations. Each LTF has two parts connected by a hinge: the proximal half-fiber is a homo-oligomer of gp34 (140 kDa) and the distal half-fiber is a hetero-oligomer of gp37 (109 kDa), gp35 (30 kDa) and gp36 (23 kDa). Both half-fibers are ~ 75 nm long and 4 nm wide: they assemble separately and then combine [1]. LTFs have been thought to be dimers of their principal constituents. We have used scanning transmission electron microscopy (STEM) mass mapping, image processing, and sequence analysis techniques to study the structures of both half-fibers and of intact LTFs isolated from mutant-infected cells. The STEM data reveal that proximal half fibers are trimers of gp34 and distal half-fibers are trimers of gp37, together with some gp36. Gel quantitation analysis of LTFs indicates a stoichiometry of gp34 : gp37 : gp36 : gp35 = 3 : 3 : 3 : 1 or 2. Correlation averaging of electron micrographs of both stained and unstained molecules resolves the LTF into two linear stacks of discreet domains. At the proximal end is a globular domain of ~ 150 kDa that becomes incorporated into the baseplate. This is followed by a shaft of uniform width (33 x 4nm; ~ 155 kDa), which correlates well with a cluster of quasi-repeats, each 34 - 39 residues long, in the primary sequence of gp34. The remainder of the LTF consists of 15 domains of differing sizes; of these, the one located at the hinge site (the "knee-cap" domain) bulges asymmetrically out on one side, indicating locally non-equivalent structure. We infer that this 70 kDa domain consists either of two copies of gp35 or one copy of gp35 together with some of gp36.

1. Wood, W.B. et al (1994) in Molecular Biology of Bacteriophage T4, p. 282- 290.

M-AM-L8

Structural Study on HIV V3 Loops

Paolo Catasti (1,2), E. Morton Bradbury (2) and Goutam Gupta (1)
(1) Theoretical Biology and Biophysics Group and (2) Life Science Division, Los Alamos National Laboratory, Los Alamos, NM 87545

The surface of human immunodeficiency virus (HIV) is studded with several copies of a glycoprotein, gp120. A segment of gp120 is the principal neutralizing determinant (PND) often targeted for vaccine development. The PND resides inside the third variable (V3) loop of gp120. However, amino acid sequence variability of the V3 loop eludes any success in vaccine development.

The elusive nature of the V3 loop calls attention toward the effect of amino acid sequence variation on the structure. An attempt is made to explore these structural aspects by combining 2D NMR spectroscopy and molecular modeling of various V3 loops.

Four different V3 loop sequences are chosen to determine the effect of amino acid sequence variation on the structure of the V3 loop.

```
V3-MN       :CTRPNYNKRKRIHIGPGRAFYTTKNIIGTIRQAHC
V3-RF       :-----N-T--S-TK----VI-A-GQ---D--K---
V3-Florida  :------YT--G-R------V-AAEK---D--R---
V3-Haiti    :-----D-T--S-PM---K---A-GD---N------
```

Two structural properties are of importance: namely, (i) the global tertiary folding of the V3 loops and (ii) the local structure of the PND. An understanding of the V3 loop would be useful in vaccine development.

M-AM-L9

THE ROLE OF THE GANGLIOSIDE G_{D1a} AS A RECEPTOR FOR SENDAI VIRUS. ((R.M.Epand‡, S.Nir|, M.Parolin‡, and T.Flanagan⊥))
‡Dept. of Biochemistry, McMaster University, Hamilton, ON, Canada, L8N 3Z5, |Faculty of Agriculture, Hebrew University, Rehovot 76100, Israel, ⊥Dept. of Microbiology, SUNY, Buffalo, NY 14214.

The ganglioside G_{D1a}, which serves as a receptor for Sendai virus, also affects lipid polymorphism as determined by ^{31}P NMR. The ganglioside promotes the formation of isotropic structures in monomethyl dioleoylphosphatidylethanolamine. G_{D1a} also raises the bilayer to hexagonal phase transition temperature of this lipid. The effects of G_{D1a} on the kinetics of viral fusion can be understood on the basis of its role in facilitating the binding of Sendai virus to target membranes as well as its effects on membrane physical properties. Fusion of Sendai virus with liposomes composed of egg phosphatidylethanolamine is particularly sensitive to the presence of ganglioside. In the absence of ganglioside no fusion is observed due to the absence of virus binding to the target membrane. Between 2 and 6 mol % G_{D1a} in egg phosphatidylethanolamine liposomes there is a marked increase in the rate constant of binding of the virus to the liposomes but a decrease in the fusion rate constant. The ganglioside enhances virus binding to liposomes of all the compositions studied, but the fusion rate constant is either unaffected or reduced. In the systems studied, the enhanced formation of isotropic structures in liposomes containing the gangliosides does not enhance the kinetics of the actual fusion reaction.

LIGHT-DEPENDENT PROTEINS: FUNCTION AND STRUCTURE

M-PM-Sym-1

THE STRUCTURE OF RHODOPSIN OBTAINED BY CRYO-ELECTRON MICROSCOPY TO 7 Å RESOLUTION
((G. F. X Schertler, V. M. Unger and P. A. Hargrave))
All members of the family of G-protein coupled receptors are expected to have the same basic structure in the membrane-embedded part of the protein. Rhodopsin is available from natural sources in reasonable quantities for crystallisation. Two dimensional crystals of bovine and frog rhodopsin have been obtained either by addition of lipids to purified rhodopsin and removal of the detergent or by extraction of frog photoreceptor disk membranes with Tween detergents. Three independent projection structures from bovine $p22_12_1$ and frog rhodopsin p2 and $p22_12_1$ crystals have been obtained. The identity of all three projection maps eliminated any possibility of the structure being affected by crystallisation. A first low resolution 3D structure of bovine rhodopsin was obtained from tilted images of the bovine rhodopsin $p222_1$ crystals (Unger and Schertler Biophys J submitted) and more recently the structure of frog rhodopsin was obtained at improved resolution from the p2 crystal form in three dimensions. In the higher resolution map of frog rhodopsin the tilts of all helices can be deduced. In particular the overall tilt of the more tilted helices is well defined in the frog rhodopsin structure. Baldwin ((1993) EMBO J 12 (4) : 1693-1703) deduced from a detailed analysis of G-protein coupled receptor sequences a set of structural constraints and a possible packing for the helices. These constraints provide an expectation for the environment of each helix and they have been used to make a tentative sequence assignment of the 7 helices in the projection map of bovine rhodopsin (Schertler et al. (1993). Nature 362 (6422) : 770-772). These constraints suggest the possible identity of particular tracks of density now in the 3D-maps of frog and bovine rhodopsin. Helices 1, 2, 3 and 5 are tilted and they form an arc through the center of the molecule. They are flanked by helix 4 on one side, and helices 6 and 7 on the other side, which are approximately perpendicular to the membrane.

M-PM-Sym-2

EXPLORING RHODOPSIN STRUCTURE AND DYNAMICS WITH SITE-DIRECTED SPIN LABELING ((Wayne L. Hubbell[1], Zorheh T. Farahbakhsh[1], Kevin D. Ridge[2], Ke Yang[2], Dave Farrens[2], John Resek[2] and H. Gobind Khorana[2])) [1]Jules Stein Eye Institute and Department of Chemistry and Biochemistry, UCLA, Los Angeles, CA; [2]Departments of Chemistry and Biology, MIT, Cambridge, MA.

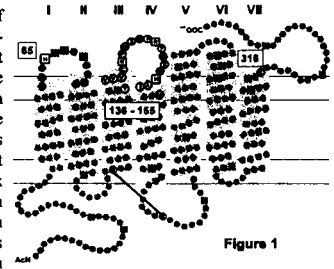

Figure 1

Twenty single-cysteine substitution mutants of rhodopsin in the sequence 136-155, a transducin binding region, and a double mutant containing cysteines at both 65 and 316, were prepared (Fig.1). Each site was modified with a sulfhydryl-specific nitroxide reagent, and the EPR spectra were analyzed. The results demonstrate that: (i) helix III extends to at least residue 140, and ~75% of the helix surface in this region is in contact with protein rather than lipid; (ii) the membrane/solution interface intersects rhodopsin near residues 138 and 152 (Fig. 1); (iii) photoexcitation produces localized changes in tertiary interaction of helix III on a millisecond time scale; (iv) residues 316 and 65, although distant in sequence, are ≤10Å apart in the rhodopsin structure as judged by dipolar interactions between nitroxides at these sites. This demonstrates the close proximity of helices I and VII in the structure, and fixes their relative position along the membrane normal; (v) photoexcitation of rhodopsin results in an increase in distance between 316 and 65, and presumably between helices I and VII. A simple model in which helices III and VII move outward upon deprotonation of the retinal Schiff base accounts for the data.

M-PM-Sym-3

FUNCTION AND STRUCTURE OF REACTION CENTER. ((H. Michel))
Max Planck Inst. for Biophys., Frankfurt.

M-PM-Sym-4

FUNCTIONAL CHARACTERIZATION OF REACTION CENTER MUTANTS.
((C.C. Schenck)) Colorado State Univ.